




Cite this: *Lab Chip*, 2026, 26, 1682

## Single-cell protein profiling energized by microfluidic technology

Ruizhe Yang,<sup>a</sup> Qingyu Ruan,<sup>\*a</sup> Wenshang Guo,<sup>a</sup> Haicong Shen,<sup>b</sup> Xiaoye Lin,<sup>b</sup> Yingwen Chen,<sup>b</sup> Ye Tao,<sup>a</sup> Chaoyong Yang <sup>c</sup> and Yukun Ren <sup>\*a</sup>

Single-cell protein profiling furnishes exclusive insights into understanding and describing phenotypic heterogeneity in large populations, garnering significant attention from researchers. However, investigating protein information at single-cell resolution has presented significant challenges on account of the small size of cells, low abundance of proteins and scarcity of sensitive analytical methods. Microfluidics has emerged as a powerful platform for single-cell protein profiling because it enables efficient single-cell isolation, high-throughput processing of small-volume samples, and integrated microscale reactions in a user-friendly format. This review provides a broad perspective on the leading-edge microfluidic platforms for single-cell protein profiling. It showcases different microfluidic layouts for single-cell separation and explores how cutting-edge analysis techniques are integrated with these platforms for protein profiling. Furthermore, the potential challenges and future trends of microfluidics-based single-cell protein profiling are presented and evaluated.

Received 8th September 2025,  
Accepted 30th December 2025

DOI: 10.1039/d5lc00854a

rsc.li/loc

<sup>a</sup> State Key Laboratory of Robotics and System, School of Mechatronics Engineering, Harbin Institute of Technology, Harbin 150001, P. R. China.

E-mail: qyruan@hit.edu.cn, rykhit@hit.edu.cn

<sup>b</sup> The MOE Key Laboratory of Spectrochemical Analysis & Instrumentation, The Key Laboratory of Chemical Biology of Fujian Province, State Key Laboratory of Physical Chemistry of Solid Surfaces, Collaborative Innovation Center of Chemistry for Energy Materials, Department of Chemical Biology, College of Chemistry and Chemical Engineering, Xiamen University, Xiamen 361005, P. R. China

<sup>c</sup> Institute of Molecular Medicine, Renji Hospital, Shanghai Jiao Tong University School of Medicine, Shanghai 200127, China

## Introduction

Cellular heterogeneity, encompassing variations in morphology, cellular functions, and molecular identities, holds an essential position in diverse biological processes, such as cell differentiation,<sup>6–8</sup> disease progression,<sup>9,10</sup> and cell metabolism.<sup>13,14</sup> With advancements in cellular component processing and profiling, previously undetected heterogeneity within cell populations and complex tissues have been



**Qingyu Ruan**

Qingyu Ruan received his Bachelor's degree in Chemistry from Xiamen University in 2015 and a Ph.D. degree in Energy Chemistry from Xiamen University in 2021. From 2021 to 2023, he was a postdoctoral researcher at the National University of Singapore and he is now an Associate Professor at the School of Mechatronics Engineering, Harbin Institute of Technology. His current research focuses on the development of

integrated microfluidic devices for single-cell analysis, single-molecule detection, and clinical diagnosis.



**Yukun Ren**

Yukun Ren is a Professor at the State Key Laboratory of Robotics and Systems at Harbin Institute of Technology, China. He received his Ph.D. degree and Bachelor's degree of Engineering degree from the School of Mechanical Engineering at Harbin Institute of Technology in 2011 and 2006, respectively. Dr. Ren was awarded the National Ten-thousand Talents Program in 2021. His research interests include the fundamentals and

applications of microfluidics, with a special interest in electrokinetics, droplets, dielectrophoresis, soft robots and point-of-care testing (POCT). He has published more than 140 papers in international journals and obtained 20 patents.

discovered. However, accurately classifying cells remains challenging due to the substantial difficulties inherent in characterizing the properties of individual cells. Single-cell omics provides exclusive insights into understanding and describing cellular heterogeneity and has seen dramatic advances within the past decade.<sup>30</sup> Numerous research studies have been presented in conjunction with the rapid development of innovative technologies, paying attention to the profiling of important biomolecules in individual cells, including DNAs,<sup>33</sup> RNAs,<sup>34</sup> proteins,<sup>37</sup> and metabolites.<sup>39</sup> Deeper insight into single-cell omics enables the discovery of novel results and the advancement of clinical applications grounded in the phenotypic identity of cells.

Proteins are crucial due to their roles in forming the cellular cytoskeleton and structures, as well as their involvement in essential cellular processes. By serving as intermediaries that connect gene expression to cellular functions, proteins can offer valuable insights into cellular behaviors and phenotypic identities. Therefore, analyzing the composition and dynamics of proteins is crucial for the elucidation of molecular pathways underlying cellular processes and disease progression. Furthermore, gaining a thorough understanding of biological processes and diseases necessitates measuring protein expression at the single-cell level.<sup>30,40</sup> Considering this reason, single-cell protein profiling has emerged as a critical necessity for uncovering pivotal features in biological processes of single cells. In this work, single-cell protein profiling refers to the systematic and multiplexed characterization of proteins in individual cells, including quantitative measurements of protein expression and protein states such as post-translational modifications and interaction-related features, enabled by microfluidic handling and integrated analytical readouts. This capability offers a quantitative framework for understanding cellular heterogeneity based on protein-level measurements.<sup>41,42</sup>

Nevertheless, profiling the proteins of individual cells remains a significant challenge in terms of efficient sample preparation and reliable signal outputs as a consequence of the low protein abundance, the intricacy of the required sample processing, and the absence of powerful analytical tools. The primary challenge of the low abundance in individual cells necessitates the utilisation of highly sensitive assays in proteomic analysis. The routine approaches for proteome analysis, such as mass spectrometry (MS)<sup>43</sup> and microarray,<sup>44</sup> lack adequate signal amplification and enough sensitivity for detecting low-abundance proteins in single cells. Secondly, in single-cell measurements, it is crucial to handle samples with high precision, as even minor analyte losses, which might be overlooked in cell population-based methods, can cause significant fluctuations at the single-cell level. A great deal of effort has been invested by researchers to tackle these barriers. This has involved employing low-binding sample tubes<sup>45</sup> and utilizing “one-pot” digestion protocols to minimize total surface exposure.<sup>46,47</sup> Third, unlike for single-cell nucleic acid analysis, powerful tools for single-cell protein analysis are still lacking. Fluorescence

microscopy and flow cytometry (FCM) have been employed for measuring single-cell protein levels.<sup>48</sup> However, the spectral overlap of the commonly used fluorescent labels restricts these imaging-based techniques from detecting numerous proteins in a single sample.<sup>49</sup> Consequently, to facilitate single-cell protein profiling, novel methodologies with enhanced detection sensitivity, enhanced sample processing efficiency, and multiplexing capability are required.

Microfluidic techniques have recently accelerated the rapid expansion of single-cell protein profiling.<sup>50,51</sup> It is capable of providing extremely efficient isolation and processing of numerous single cells in a miniaturised device, significantly simplifying workflows, improving integration and throughput, and enhancing detection sensitivity. Single-cell protein profiling has been achieved using a microchip that manages cell separation, processing, and the quantification of proteins.<sup>52</sup> This review outlines how the recent advancements in microfluidic technologies have been employed to upgrade single-cell protein profiling through representative platform architectures and integrated analytical readouts (Fig. 1). Firstly, we examine the various microfluidic layouts applied to isolate and manipulate single cells for protein analysis. Following this, we explore the principles and representative applications of microfluidic platforms coupled with other cutting-edge analytical instruments for single-cell protein analysis and compare the utility of these methods. Finally, we discuss future developments and potential challenges of microfluidic single-cell protein profiling technologies.

## Microfluidic approaches for single-cell separation

Effective separation of single cells is fundamental for accurate protein analysis. Currently, a variety of microfluidic layouts have been established for single-cell handling based on a range of fundamental fluid management technologies, including traps, valves, droplets, microwells and fields.<sup>53–55</sup> Compared with conventional isolation methods (*e.g.*, limiting dilution, micromanipulation, and laser microdissection), microfluidic approaches enable more controlled handling with reduced dilution and facile integration with downstream assays.

Notably, rare-cell samples such as circulating tumor cells (CTCs) pose additional challenges relative to typical single-cell inputs because targets are extremely sparse and embedded in a high-background matrix (whole blood). Therefore, clinically oriented workflows often incorporate an explicit enrichment or pre-concentration step prior to downstream single-cell proteomic analysis. Immunocapture strategies are widely used to suppress leukocyte background and improve purity; a representative example is the EpCAM-functionalized CTC-chip that isolates CTCs directly from patient blood.<sup>56</sup> To reduce marker bias, label-free size-based enrichment is frequently adopted; for instance, spiral inertial

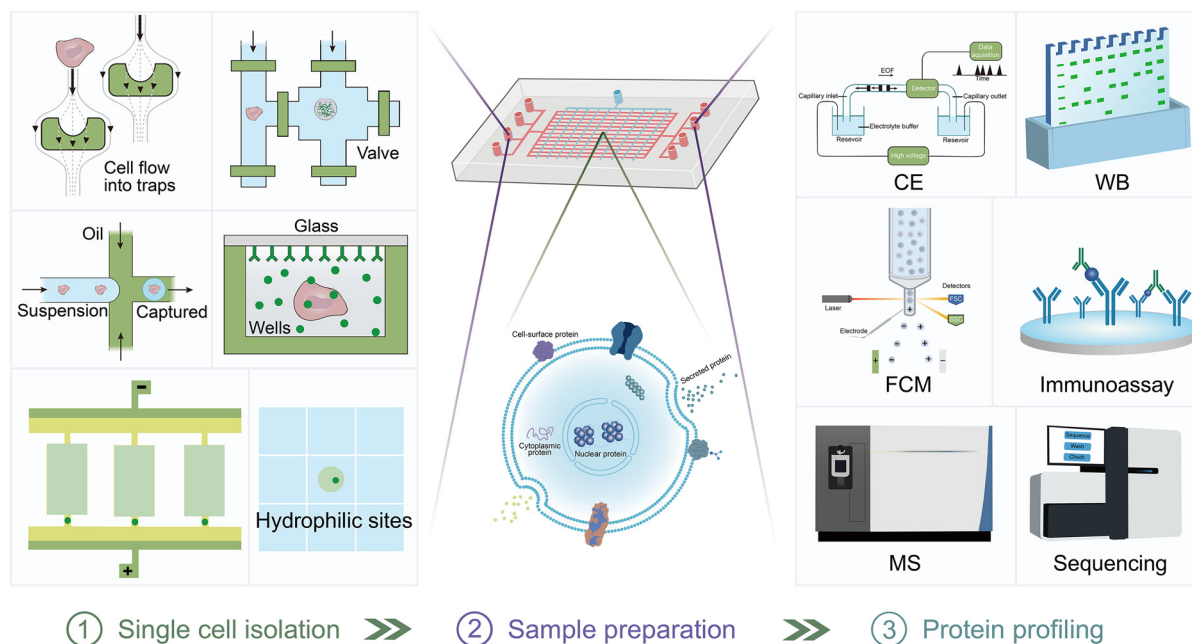


Fig. 1 Overview of various microfluidic systems for protein measurements in single-cell protein profiling.

microfluidics has been demonstrated for ultra-fast, label-free CTC enrichment from clinically relevant blood volumes.<sup>57</sup> Beyond simple size filtration, deterministic lateral displacement (DLD) offers geometry-defined, continuous fractionation and has been integrated into clinically oriented CTC workflows; the antigen-independent CTC-iChip combines DLD-based debulking with inertial focusing and magnetic depletion to isolate rare CTCs from blood.<sup>58</sup> Dielectrophoresis (DEP) provides an additional marker-free handle based on dielectric properties; for example, an optically induced DEP (ODEP) microfluidic system has been integrated with flow-velocity control to further isolate and purify CTCs after an initial conventional enrichment step, enabling selective manipulation of rare tumor cells under continuous-flow conditions.<sup>59</sup>

These rare-cell workflows impose tighter downstream constraints than bulk-cell analyses: even minor blood carryover can dominate analytical background. Moreover, the low protein mass per cell amplifies losses due to adsorption and sample handling in MS-based proteomics, motivating nanoliter-scale, low-loss processing formats (*e.g.*, the nested nanoPOTS (N2) chip<sup>60</sup>). In addition, mass cytometry readouts can be affected by channel spill over, which typically requires appropriate compensation. In the following section, we discuss representative microfluidic platforms for single-cell protein profiling, focusing on their working principles and relative merits.

### Traps

The hydrodynamic-based cell trap represents a structural system whereby single cells are extracted from a cell suspension flow when they become obstructed by a

microscale structure.<sup>61</sup> As a cell suspension stream traverses the structure, cells within the flow are directed and channeled towards the weir. Once a single cell fills the weir, the flow resistance rises sharply, diverting the main flow and directing subsequent cells towards the slots on either side (Fig. 2A). Recent years have seen transformative improvements in hydrodynamic trap architectures for single-cell capture. Nguyen *et al.*<sup>62</sup> devised a novel three-micropillar (3  $\mu$ PF) hydrodynamic trap that interleaves micropillars to distribute shear forces and enhance cell exposure to culture medium, thereby enabling prolonged dynamic culture with reduced mechanical collisions, as confirmed by finite-element simulations.

### Valves

A valve-based platform typically comprises soft elastomeric membranes that function as pressure valves that can confine a single cell in the chamber by blocking the flow pathways.<sup>63,64</sup> When air or liquid is applied to the interior of the perpendicular valve, a bulge is raised towards the channel, forming a separated chamber (Fig. 2B). In this way, a single cell flowing through this area can be captured. Additional valves can be used to mix or transfer reagents for downstream protein analysis. Valve-based microfluidic platforms are well-suited for executing intricate single-cell molecular profiling workflows. They can be easily integrated with various sensors and detection systems, allowing for the simultaneous isolation, reaction, and measurement of hundreds to thousands of single cells. One of the classical cases is the platform named Fluidigm C1, developed by Genshaft and coworkers.<sup>65</sup> By controlling the valves, the fluidic channel is separated into several micro-chambers

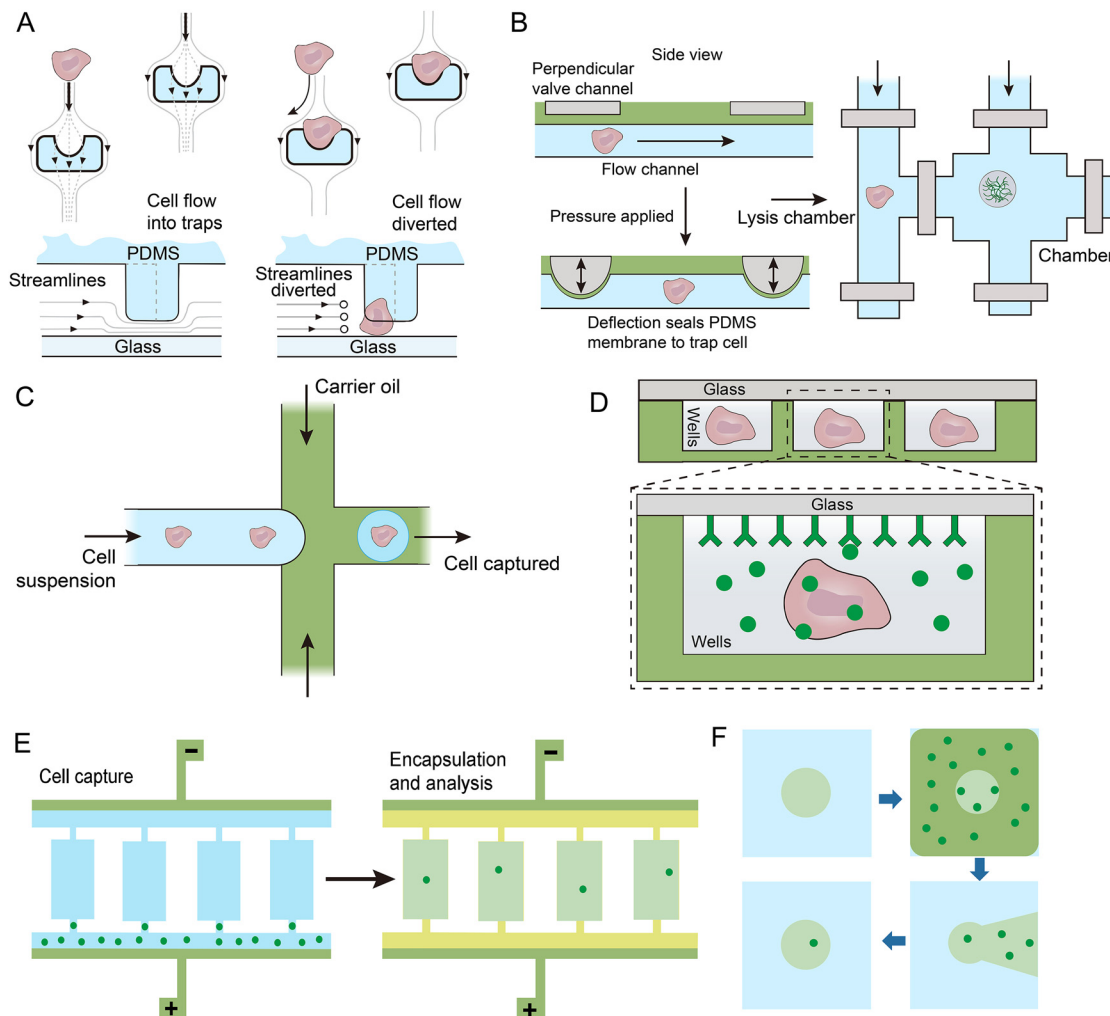


Fig. 2 Microfluidic methods for single-cell separation: (A) traps, (B) valves, (C) droplets, (D) microwells, (E) DEP, and (F) EWOD devices.

used for single-cell capture, lysis, and protein analysis, respectively. Thus, a series of reactions for single-cell analysis can be integrated on only one chip.

### Droplets

Droplets have been used to compartmentalize and study single cells since the 1950s.<sup>66,67</sup> Usually, cells are separated from each other by water-in-oil droplets, which provide an independent enclosed microenvironment for each cell, enabling the target signals to be enriched separately and avoiding contamination (Fig. 2C). The flow-focusing structure is most commonly used in droplet-based microfluidic devices, providing higher pressure to the continuous aqueous phase, which reduces size differences and enhances droplet separation. The droplet-based platform can generate thousands of droplets per second with the volume ranging from femtoliter to nanoliter according to the design and flow velocity, allowing for high-throughput single-cell analysis.<sup>40,68</sup> However, due to Poisson-based cell distribution and limited control within individual droplets, the droplet workflow can

be inherently disordered. Therefore, hybrid microfluidic approaches combining droplet-based encapsulation with other compartmentalization or control modalities have emerged as effective solutions to the limitations inherent in droplet-only systems.

Hybrid platforms that integrate droplet microfluidics with microwell arrays or pneumatic microvalve circuits enable deterministic cell loading and fluid manipulation, thereby substantially reducing the stochastic variation and doublet contamination associated with Poisson-distributed cell encapsulation. For example, a recent platform integrates droplet generation, incubation, and phenotypic sorting on a single chip: droplets are formed first, then pneumatic microvalves route selected droplets through modules that enable precise capture, buffer exchange, and sorting according to fluorescence or other criteria, thereby enhancing processing accuracy and flexibility.<sup>69</sup>

More recent innovations have paired droplet microfluidics with external physical fields—including fluorescence-activated droplet sorting (FADS), acoustic waves, electric or magnetic fields, and picoinjection—to impart active control

post-encapsulation. A notable example is the spinDrop platform, which first applies in-line FADS to enrich droplets containing viable single cells or target nuclei, and then uses picoinjection to add reagents such as lysis buffer and reverse transcription enzymes directly into selected droplets.<sup>70</sup> This multi-step, field-driven workflow yields a fivefold increase in gene detection rates, while halving the background noise compared to conventional inDrop approaches. These hybrid strategies have become common practice in single-cell proteomics applications.

### Microwells

The microwell-based platform usually comprises high-density microwells fabricated onto the surface of glass or polydimethylsiloxane, serving as individual reaction microchambers for single cells.<sup>71–76</sup> A cell suspension characterized by statistical sparsity is usually deposited into the microwells by gravity. To ensure isolated environments and prevent cross-contamination, each well can be sealed, for example, with a glass coverslip or an oil overlay (Fig. 2D). The Love group developed a soft lithographic microwell-based method for the rapid selection of single cells producing antigen-specific antibodies.<sup>71</sup> In this method, a glass slide covalently immobilized with capture-antibody creates an isolated environment for reactions and enables the detection of proteins liberated from cells in each well. A significant advantage of microwells is their ability to operate easily and efficiently in a highly parallel manner. Alternatively, centrifugation or dielectrophoresis can be combined with microwell-based platforms to elevate the efficiency of single-cell separation.<sup>77</sup>

### Field

Due to the advantages of precise control, flexible manipulation, and contactless manner, field-based microfluidic methods are widely used for single-cell analysis, including electric, optical, magnetic, and acoustic microfluidics.<sup>78</sup> Among these methods, electrical techniques are more broadly employed due to several advantages. Electrical fields do not require labeling, are easier to handle, and typically exert less physical pressure on cells compared to other methods. The two main methods of electronically controlled single-cell separation based on electrical control are dielectrophoresis (DEP) and electrowetting-on-dielectric (EWOD).

Dielectrophoresis (DEP) was the first electrical method developed for single-cell separation. It leverages the difference in conductivity between the cell and its surrounding medium to manipulate and separate individual cells.<sup>79</sup> In the DEP system, specific voltages and frequencies are used to generate gradient electric fields that induce polarizable particles to move towards regions of higher (positive DEP) or lower (negative DEP) electric field gradients. This approach enables single-cell separation and selective capture derived from the dielectric properties of the cells. Additionally, when combined with conventional microfluidic

microchambers, it allows for the dispersion of individual cells into separate chambers for subsequent analysis (Fig. 2E). Wu *et al.* described a planar chip integrating cell capture microarrays with positive dielectrophoresis (pDEP), which achieved single-cell pairing efficiencies exceeding 70%.<sup>80</sup> This device holds significant potential for further studies on cell–cell interaction. Qin and colleagues developed a self-digitization dielectrophoretic (SD-DEP) chip hybrid with a microchamber array structure.<sup>81</sup> In this device, cells were captured by pDEP at the inlet of each chamber and then sequentially passed into each reagent for subsequent reactions. To prevent contamination, the chambers are encapsulated by passing immiscible oil phases between reaction steps. This method enables the integration of all processing steps for single-cell isolation, treatment and subsequent nucleic acid analysis. More recently, Li and Anand have developed an improved single-cell capture system utilizing arrays of bipolar electrodes, which achieves an 84.4% efficiency in capturing single cells into nanoliter chambers.<sup>82,83</sup>

EWOD technology, also known as digital microfluidics (DMF), facilitates the management of picoliter-to-microliter droplets with programmatic control, making it highly suitable for integrated single-cell analysis.<sup>84,85</sup> The most efficient method for single-cell analysis using DMF is limiting dilution. This method is implemented by dividing droplets containing several cells into multiple sub-droplets, to ensure that each sub-droplet contains only one cell.<sup>86</sup> Furthermore, EWOD can isolate single cells by altering the local hydrophilicity or hydrophobicity of the EWOD electrode surfaces. When droplets pass over the hydrophilic sites, the action of surface tension leaves behind a smaller sub-droplet at the site, thereby achieving passive isolation of single cells (Fig. 2F). The Wheeler group further showed the digital microfluidic isolation of single cells for -omics (DISCO), allowing the user to pick out distinct individual cells from a heterogeneous population and collect the cellular contents.<sup>26</sup> The integration of EWOD technology with conventional microfluidic systems enables precise hydrodynamic single-cell isolation through microstructures on functionalized electrode substrates. Ruan *et al.* designed wettability-based hydrodynamic traps, called butterfly structure, combining hydrodynamics with surface wettability techniques to furnish high single-cell capture efficiency.<sup>87</sup> The butterfly structure is designed to concentrate cells in the suspension flow into the weir at its center. When a single cell occupies the weir, the increased flow resistance redirects subsequent cells to the sides. Concurrently, the hydrophilic sites beneath the butterfly microstructure retain the captured cells within the weir for further analysis. More recently, Samlali *et al.* developed a three-layer microfluidic chip for single-cell manipulation, comprising a patterned indium tin oxide (ITO) electrode, a silicon nitride dielectric layer, and a PDMS microchannel network.<sup>88</sup> In this system, cells are hydrodynamically captured in the upper microchannel and encapsulated into picoliter-scale droplets. Programmable

electrowetting actuation triggers controlled cell release through dielectrophoresis or droplet fusion, achieving precise single-cell isolation.

Although electric field-based methods offer several advantages, such as simple operation, high capture efficiency, minimal cell damage, and automated control, they still face significant limitations. The need for specific electrode designs and the limitation of electrode numbers are the primary constraints on the widespread use of this technology. Addressing these issues represents the principal avenues for further advancement.

## Microfluidic approaches for single-cell protein profiling

### Microfluidic capillary electrophoresis

Capillary electrophoresis (CE) is a separation and detection tool that has been demonstrated to be highly efficient in separating analytes and to have remarkable sensitivity in ion detection. This method performs protein analysis utilizing a high-voltage electric field within a micro-scale capillary. CE offers advantages such as efficient separation, easy integration, and strong

compatibility with single cells, making it highly promising for single-cell protein analysis. However, conventional CE systems face challenges, including poor reproducibility, prolonged separation times, and restricted geometrical dimensions. Microfluidic CE has emerged as a solution to these limitations by the automation and integration of single-cell injection and manipulation. This technology enables the online separation and detection of diverse constituents at the individual cell scale. Zare's group pioneered an integrated microfluidic CE device for single-cell protein analysis.<sup>89</sup> This device encompasses four key functionalities: cell manipulation, precise gauging and delivery of lysis solutions, online cell lysis and derivatization, and separation and laser-induced fluorescence detection of derivatized proteins. Building on this platform, the team further advanced the multistate valve technology to quantify low-copy-number proteins from single mammalian and insect cells using single-molecule fluorescence counting (Fig. 3A).<sup>1</sup> Although integrated microfluidic CE shows promise for single-cell protein analysis, its application still faces challenges like nonspecific adsorption, low throughput, and a limited number of protein assays. To overcome these obstacles, several improvements have been proposed: surface modifications to prevent nonspecific

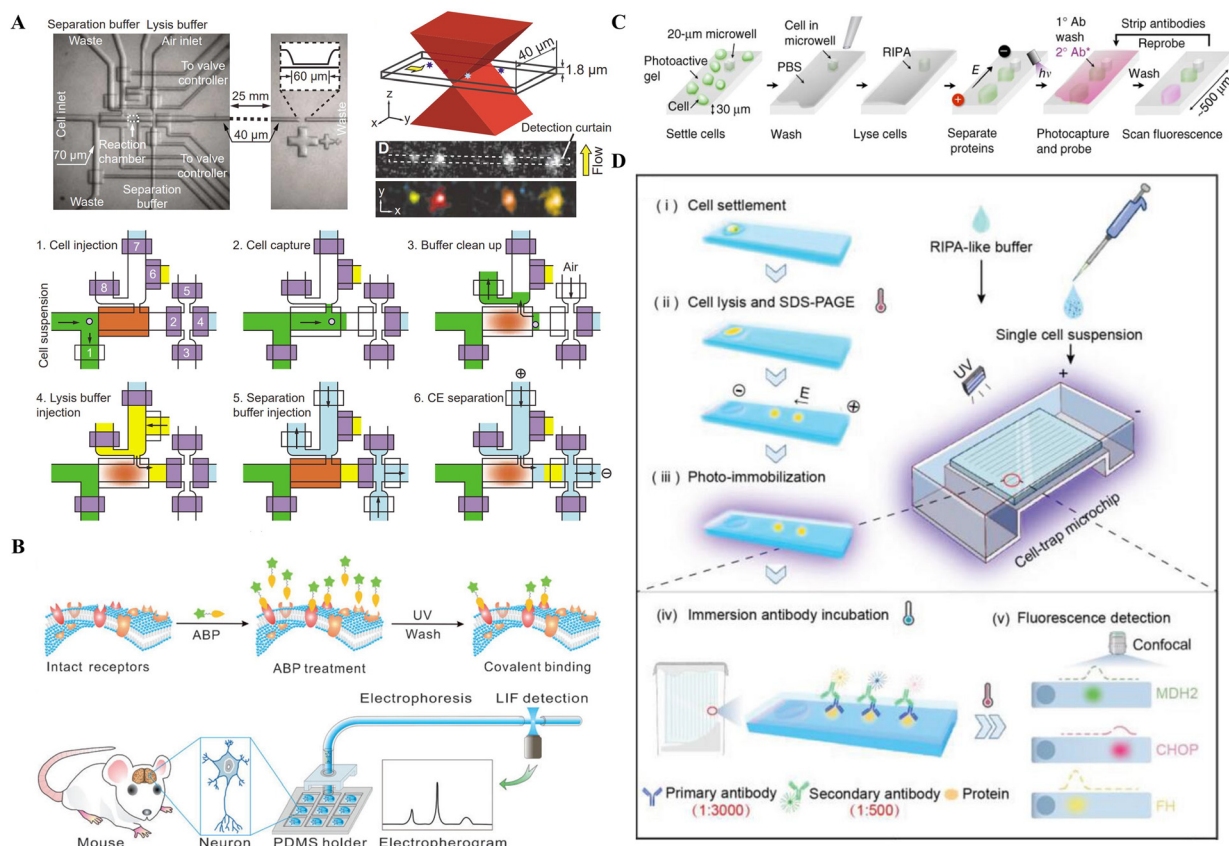


**Fig. 3** Microfluidic electrophoresis for single-cell protein analysis. (A) Schematic of the integrated microfluidic CE chip for single-cell analysis. Reproduced with permission.<sup>1</sup> Copyright 2007, The American Association for the Advancement of Science. (B) Illustration of the SCCP strategy. Reproduced with permission.<sup>22</sup> Copyright 2014, WILEY-VCH Verlag. (C) Principle and workflow of the single-cell Western blotting. Reproduced with permission.<sup>27</sup> Copyright 2014, Springer Nature. (D) Schematics of tc-sc Western based on ANP hydrogel: single-cell settlement, cell lysis, protein electrophoresis, UV immobilization of proteins *in situ*, antibody incubation, and in-gel fluorescence detection of immobilized proteins. Reproduced with permission.<sup>28,29</sup> Copyright 2024, WILEY-VCH Verlag.

protein adsorption, parallel single-cell CE to increase detection throughput, and multicolour fluorescence detection to enhance multiplexing capabilities.<sup>90–94</sup>

In addition to antibody-based methods, small molecule fluorescence probes have been successfully applied for single-cell protein detection. Liu's group introduced a chemical cytometry approach utilizing CE technology, presenting the single-cell chemical proteomics (SCCP) method for the identification of membrane proteins in individual primary neurons (Fig. 3B).<sup>22</sup> Functional single cells were extracted from mice and labeled with high-specific activity probes. The labeled cells were then packed in individual droplets and placed in a polydimethylsiloxane (PDMS) microwell array. Subsequently, these cells were transferred one at a time into a CE system for online processing and analysis using laser-induced fluorescence (LIF). The SCCP strategy was extended to demonstrate single-cell functional protein analysis in the cytosol of two types of tumor cells, reaching a limit of detection of 0.1 pM.<sup>95</sup> More recently, Shi *et al.*<sup>96</sup> introduced a highly sensitive and selective CE-LIF analysis to measure low-copy-number intracellular proteins in single cells using a cheap fluorescence detector and a BV605 probe. They achieved a limit of detection of 7 molecules in a 91 pL reaction volume. However, the susceptibility to protein adsorption on the capillary wall poses a significant challenge to the sensitivity and stability of detection in CE-based microfluidic methods, limiting practical applications.

### Microfluidic gel electrophoresis

While microfluidic CE has made some progress, it is difficult to perform protein quantification and lacks the scalability to perform large amounts of parallel electrophoretic analysis. Western blotting (WB), an influential protein analytical method, combines high-resolution gel electrophoresis and immunochemical analysis, offering advantages such as high scalability, high sensitivity, and quantifiability.<sup>97,98</sup> Single cell western blots (scWestern) have been presented by the Herr group (Fig. 3C).<sup>27</sup> The scWestern system comprises a microscope slide and an array of microwells constructed with a thin layer of photoactive polyacrylamide (PA) gel. Cells are captured into the microwells through gravity, followed by cell lysis. Individual cell proteins are then separated within the PA gel resulting from an electric field. After separation, proteins are immobilized in a three-dimensional PA gel by UV light, and target proteins are identified using fluorescent antibody probes. While the method's dynamic range is comparatively narrow, scWestern is comparable to FCM in sensitivity and can detect dozens of proteins through stripping and re-probing. Currently, scWestern has evolved into a crucial tool for single-cell protein profiling, attracting significant attention.<sup>99,100</sup> Recently, Li *et al.* presented a single-cell transfection analysis chip (scTAC) to highly efficiently assess transient transfection efficiency.<sup>101</sup> scTAC allows for the monitoring of exogenous gene expression of a

few thousand single cells, facilitating continuous protein expression profiling even under conditions of low-level coexistence. Grist and colleagues showed three-dimensional immunoblots for single cells, detecting intracellular proteins of a few hundred cancer cells.<sup>102</sup>

However, scWestern still faces significant difficulties for identifying low-abundance proteins and small molecular weight proteins. During the separation and immunoblotting processes, protein bands rapidly diffuse into the buffer solution, resulting in substantial loss of these proteins, thereby making them difficult to be detected.<sup>103</sup> To address these issues, the Ding group introduced an intensive single-cell immunoblotting method using a tetrazole-functionalized photoactive hydrogel (Fig. 3D).<sup>28,29</sup> The photoreactive tetrazole undergoes electrophilic addition reactions with proximal protein nucleophiles within seconds *via* click chemistry. This approach enables the capture of separated proteins swiftly and efficiently, thereby reducing excessive band diffusion and minimizing autofluorescence on the microchip. Moreover, scWestern heavily depends on fluorescence-based readouts, prone to loss of signal during multiplexed detection requiring multiple rounds of target re-labeling. Lomeli *et al.* developed scWestern with a MIBI-TOF (multiplexed ion beam imaging by time of flight) readout using metal tagging, enabling high-multiplex protein profiling.<sup>104</sup> Moreover, antibody incubation in western blotting is critical, since the access of antibodies into a wet hydrogel is impeded by a number of factors, including size exclusion, hydrophobic interaction and electrostatic repulsion. Efforts have focused on increasing antibody concentrations in gels to improve incubation efficiency in scWestern.<sup>105,106</sup> Typically, the cell capture efficiency of scWestern is very low, resulting in high cell loss. Recently, microfluidics has been integrated to enable protein analysis of individual circulating tumour cells (CTCs). The body's response to therapy is monitored by detecting multiple protein targets in individual CTCs.<sup>107</sup>

### Microfluidic flow cytometry

FCM is a classic method for analyzing proteins at the single-cell level, which can measure the fluorescence properties of labelled individual cells in a fluid as they pass through a light source. It offers many advantages such as excellent sensitivity, multiplexing capabilities, and high throughput. However, FCM instruments are not only expensive but also require trained personnel for operation and maintenance, making them costly to use. Additionally, sample preparation for traditional FCM involves enormous cells ( $>1 \times 10^6$  cells per mL), making it impractical to analyze rare and valuable samples. To address these issues, microfluidic cytometers have been involved, combining microfluidic technology with miniature detectors, enabling protein profiling at the single-cell level.

**Valve-based microfluidic flow cytometry.** The valve-based FCM is a miniaturized version of FCM integrating single-cell

sample handling on a microfluidic chip for quantifying single-cell protein expressions.<sup>108–113</sup> In general, single cells that have been either surface- or intracellularly stained are introduced into the microfluidic channel. Subsequently, these suspended single cells undergo sequential processing using an integrated laser light source and fluorescence detection device. The target protein copy number is quantified by measuring the fluorescence intensity of the

labelled single cells. As an illustration, Srivastava *et al.* went further by incorporating multi-colour flow cytometry to detect signalling events across multiple time scales and intercellular locations. This was achieved through an integrated cellular sample preparation process on a microfluidic chip that is seamlessly connected with downstream FCM (Fig. 4A).<sup>4</sup> The design quantitatively recorded changes in the fluorescence density associated with these translocation processes with

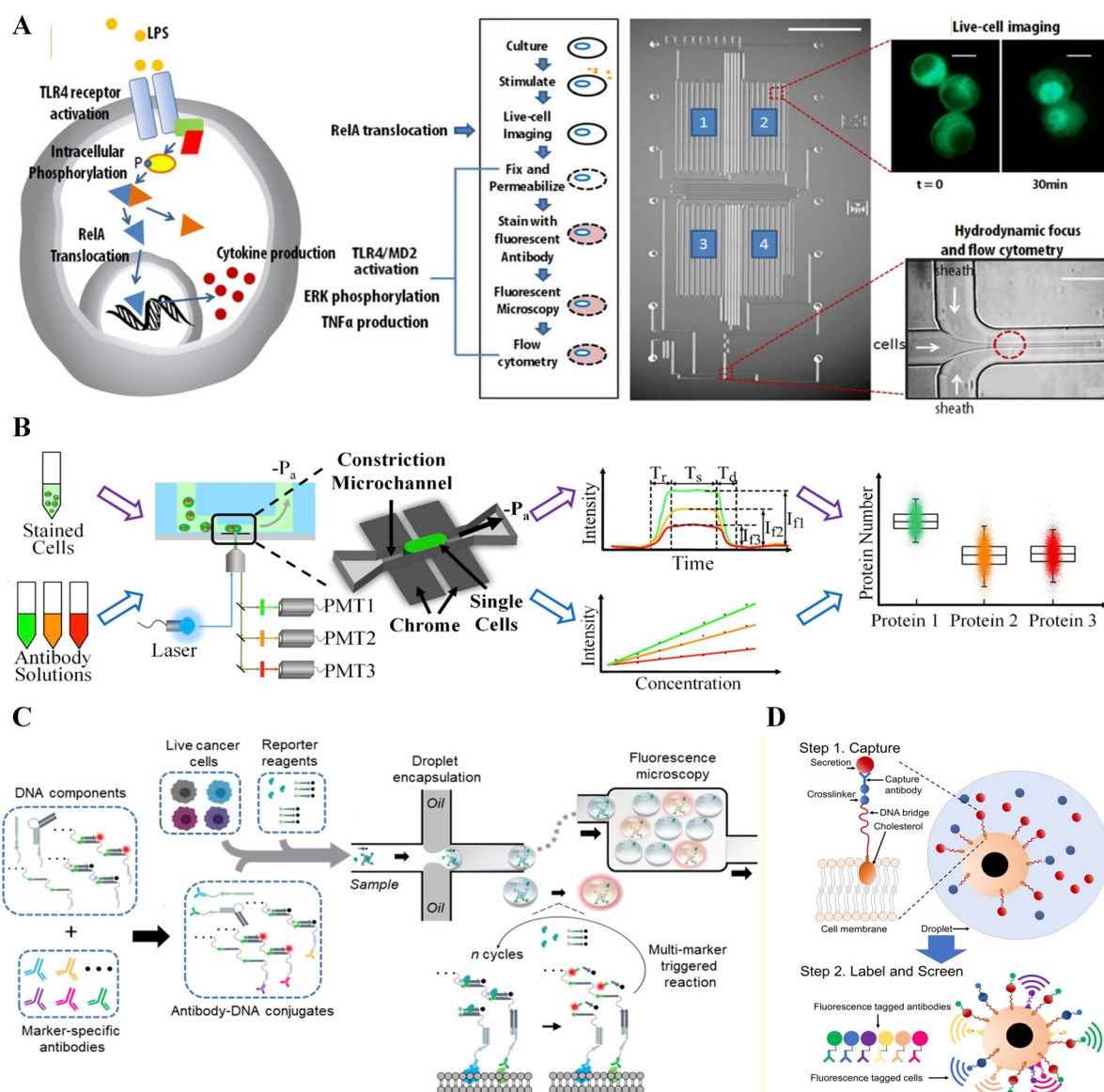


**Fig. 4** Microfluidic FCM for single-cell protein analysis. (A) Workflow of an integrated microfluidic chip for global profiling of cellular pathways at single-cell resolution. Reproduced with permission.<sup>4</sup> Copyright 2012, The Royal Society of Chemistry. (B) Schematic of the constriction microchannel-based microfluidic platform enabling high-throughput quantification of multiple types of intracellular proteins in single cells. Reproduced with permission.<sup>12,17</sup> Copyright 2020, Elsevier. (C) Overview of FDC: cells labelled by antibody–DNA conjugates mixed with reporter reagents then undergo a single-cell encapsulation process in a droplet microfluidic device, initiating an enzymatic amplification reaction in the droplet to achieve live-cell phenotypic profiling of single and multi-surface markers *via* readout of droplet fluorescence. Reproduced with permission.<sup>23</sup> Copyright 2020, the American Society Chemistry. (D) Schematic of the cell membrane immunosorbent assay based on CLAB technology. Reproduced with permission.<sup>31</sup> Copyright 2024, the American Society Chemistry.

single cell resolution by an elastomeric valve forcing flowing cells into the evanescent field. Furthermore, Liu *et al.*<sup>17</sup> developed a microfluidic flow cytometer using a constriction channel narrower than cell diameters, enabling the identification of the copy numbers of target proteins (Fig. 4B). This work presented a microfluidic platform that processed cells stained with multiplex fluorescence-labeled antibodies through constricted microchannels. It detected the resulting fluorescence signals using three photomultiplier tubes (PMT) simultaneously and translated them into the number of target protein binding sites. This innovative platform can quantify multiple intracellular proteins in the numerous individual cells, enabling efficient cell type classification based on protein expression data. Moreover, for the hydrodynamic focusing system, in contrast to conventional methods using planar microfluidic approaches,<sup>114–116</sup> stable single-stream focusing<sup>117</sup> was developed at high Reynolds numbers and high flow velocities, allowing for precise and massively parallel FCM. This advancement facilitates the seamless integration of fluid manipulation techniques with suitable optical systems.

**Droplet-based microfluidic flow cytometry.** Droplet microfluidics has also been employed in conjunction with FCM to quantify proteins in single cells.<sup>118–120</sup> Chen's group developed a series of constriction microchannel-based droplet microfluidic FCM systems, enabling high-throughput, quantitative measurements of single-cell proteins.<sup>121–123</sup> For example, in 2023, they presented a quantitative FCM platform of multiplex fluorescence detection utilizing droplet-based constriction channels for quantifying single-cell protein expression levels. Single cells stained with fluorescent probe-labeled antibodies were encapsulated with proteinase K, guanidine hydrochloride, and urea. The bound antibodies were stripped off, resulting in droplets with uniformly distributed fluorescence. These droplets, containing uniformly distributed fluorescein-labeled antibodies, deformed as they passed through a constriction microchannel. Here, the excited fluorescence signals were sampled and interpreted into protein counts based on volume equivalence in droplet measurement and fluorescence calibration. However, obtaining information on a single-cell basis for living cells is another challenge. Yang and coworkers reported a droplet microfluidic FCM strategy for single-cell phenotype tracking of living cancer cells, named FDC, which utilized a target-specific enzymatic amplification reaction (Fig. 4C).<sup>23</sup> Antibody–DNA conjugates are used in conjunction with diverse cell samples to identify specific biomarkers present on the cell surface. Using a DNA-triggered reaction activated exclusively in the appearance of several biomarkers, FDC facilitates the identification and mapping of surface markers on live cancer cells with single-cell resolution. This method enabled living cell phenotypic profiling of multiple surface markers from collections of fewer than 40 cells.

A key feature of droplet microfluidics is the simultaneous encapsulation of single cells and reagents within individual droplets. Consequently, droplet microfluidic FCM allows for the analysis of proteins secreted by individual cells, a capability not

achievable with conventional FCM.<sup>119,124–130</sup> In such system, for instance, single cells and specialized beads were encapsulated in hydrogel droplets, in which beads were engineered to attach to cytokines released by individual cells.<sup>130</sup> Next, the emulsion was broken down through gelling and washing of the droplets. These were then incubated with fluorescently labeled detection antibodies specific to cytokines attached to the beads. Following this, FCM was used to quantify the signal intensities in the beads. Shembekar *et al.* utilized this system to build a large-scale antibody screening platform with dual-colour normalized fluorescence output to identify antibodies coupled with target cells.<sup>129</sup> This enables a 220-fold enrichment after sorting 80 000 clones within only one experiment. However, the single-cell droplet microfluidic FCM assay requires co-encapsulation of single cells and biosensors in the droplets. The single-cell droplet encapsulation rate, governed by a Poisson distribution, constrains the throughput. Recently, Xu *et al.* developed a microfluidic cellular membrane immunosorbent assay based on cholesterol-linked antibody (CLAb) technology for high-throughput single-cell multiplexed secretion analysis (Fig. 4D).<sup>31</sup> Initially, CLAbs produced *via* click chemistry were attached to the cell surface by the interactions between cholesterol and lipids. These cells were then encapsulated in droplets to capture their secretions on the cell surface. Subsequently, the cells with captured secretions were de-emulsified from the droplets. The recovered cells were labeled with fluorophore-tagged antibodies in bulk to concurrently discern several surface proteins and secretions. The barcoded cells were subsequently analyzed using FCM for high-throughput single-cell secretion profiling. For illustration, this approach enabled the concurrent quantification of multiple cytokines and surface proteins in individual cells at a throughput of  $\sim 10^3$  cells per second, and it was successfully applied to analyse PBMCs from patients with nasopharyngeal carcinoma.

These droplet-based microfluidic platforms typically use multicolor systems to detect multiple proteins per cell. However, this limitation is not fundamental. By combining multicolor excitation and imaging techniques with various dyes, higher levels of multiplexing can be achieved. Nonetheless, the additional costs and complexities associated with these techniques must be considered. Therefore, a balance between multiplexing capability and cost must be struck, depending on the chosen experimental system.

### Microfluidic barcoding immunoassay

Most proteins in single cells exist in low abundance. These proteins are not detectable by conventional labelling, requiring further signal amplification for high-sensitivity and high-specificity detection. Recently, microfluidic-based immunoassay methods have been developed to enable multiplexed protein detection on a single-cell scale. These methods include microchip-based assays, single-cell barcode chip (SCBC) technology, droplet microarrays, beads-on-barcode antibody microarrays, and single-molecule array technologies, *etc.* Microfluidic barcoding immunoassays, in

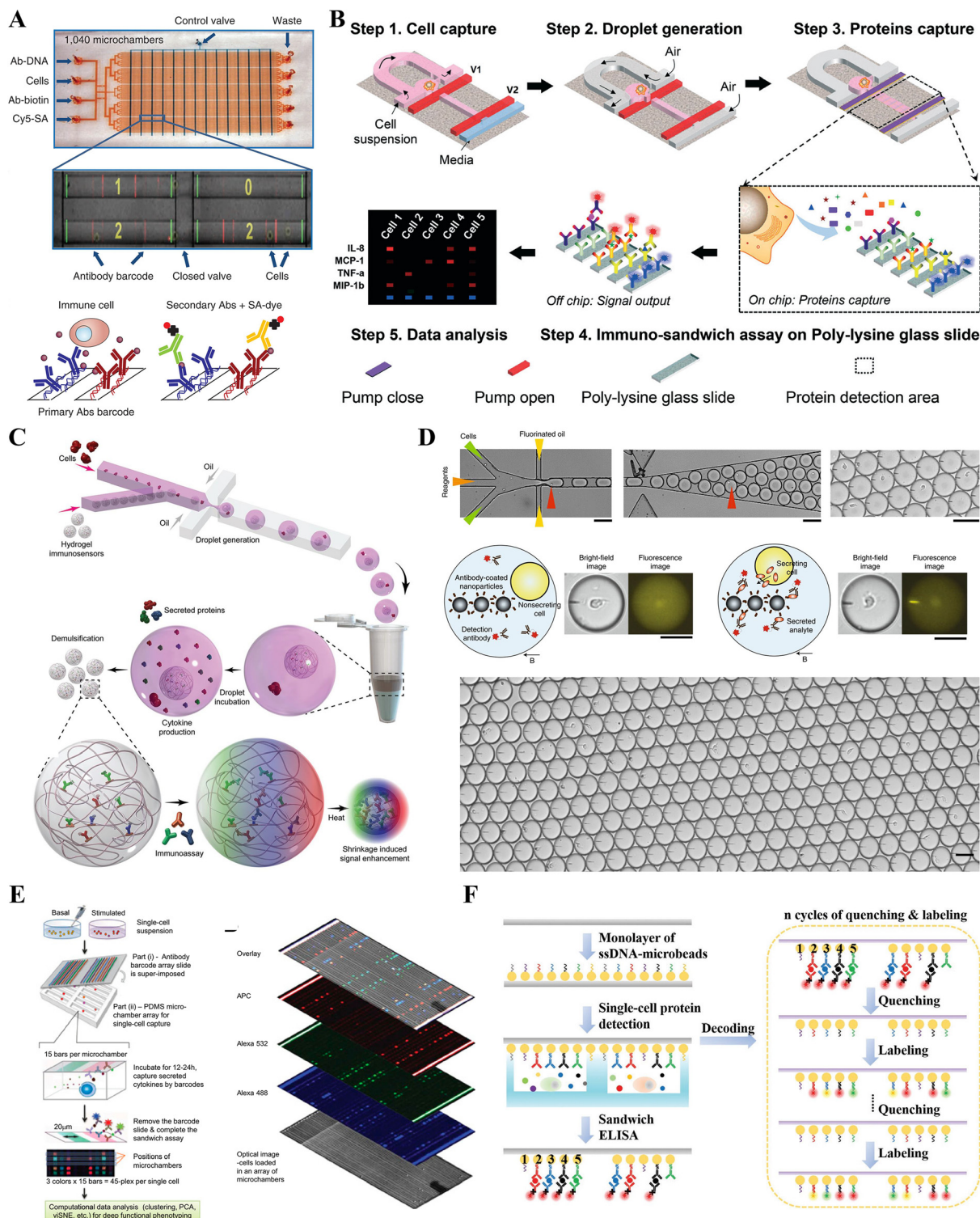


**Fig. 5** Microfluidic barcoding immunoassays for single-cell protein analysis. (A) Design of the SCBC for single-cell protein secretome analysis. Reproduced with permission.<sup>21</sup> Copyright 2011, Springer Nature. (B) Workflow of the integrated microchip platform to isolate, culture, and detect the presence of multiple proteins secreted by individual cells by fluorescence sandwich ELISA. Reproduced with permission.<sup>25</sup> Copyright 2021, The Royal Society of Chemistry. (C) A smart hydrogel microfluidic platform for the sensitive detection of single cellular protein secretion. Reproduced with permission.<sup>52</sup> Copyright 2018, Wiley-VCH Verlag. (D) Illustration of the DropMap platform. Reproduced with permission.<sup>55</sup> Copyright 2020, Springer Nature. (E) Strategy of antibodies spectral encoding and spatial encoding for single-cell multiplexed protein detection. Reproduced with permission.<sup>36</sup> Copyright 2015, National Academy of Sciences. (F) Scheme of the whole procedure for multiplexed single-cell protein detection and decoding on the encoded MIST arrays. Reproduced with permission.<sup>38</sup> Copyright 2018, Wiley-VCH Verlag.

particular, have emerged as a technique for multiplexed protein detection.

**Valve-based single-cell barcoding microchips.** The initial microchip category to use microfluidic barcoded immunoassays to profile single-cell proteins, the valve-based SCBC,<sup>21</sup> was developed by the Heath team. SCBC consists of a few thousand individually microchambers for single-cell settling, lysis, and capture of specific proteins through pre-stamped antibodies on the chamber surfaces (Fig. 5A). Employing flow restriction alongside the DNA-encoded antibody library method, the pre-printed antibody barcode array is composed of parallel stripes of distinctive antibodies. This design enables quantitative measurement through fluorescent immunosandwich assays, allowing for the absolute quantification of both single-cell cytoplasmic and membrane proteins. While limited in spectral multiplexing, the approach can be expanded by augmenting the quantity of designed antibody stripes. Khajvand and colleagues presented a droplet-based integrated microfluidic platform microfluidic platform to encapsulate individual cells efficiently for single-cell secretome analysis (Fig. 5B).<sup>25</sup> The droplet-based integrated microchip is composed of two parts: a glass substrate featuring dense antibody barcodes for immunoassay and a PDMS chip with pL-level chamber arrays for the separation of single cells. Firstly, cells were individually captured in confined picochambers based on hydrodynamics. Then, air was introduced into the channels in reverse in the role of the medium for droplet formation to separate the cells. Next, the unlocking of microvalves connected the isolated picochambers with the media channel, cells were incubated on-chip and the secreted proteins were recognized at the defined antibody bonds in each detection zone. The array of 100 pL-level chambers achieved over 80% efficiency in capturing single cells. Leveraging these microscale chambers, the platform successfully analyzes protein secretions of cancer cells sourced from both primary and metastatic sites in patients. This capability unveils significant diversity in secretion patterns among the cells. While the SCBC platform, the first pump-based integrated platform for multiplexed protein analysis, has achieved significant improvements in multiplexing capability and high sensitivity, it is still limited by the complexity of antibody barcoding construction and multiple pumps/valves operation.

**Droplet-based single-cell barcoding microchips.** Droplet microfluidics enables high-throughput quantification of single-cell proteins through dispersing cell populations into individual cells rapidly, overcoming the throughput limitation of valved-based microfluidics. Hsu *et al.* reported a smart hydrogel droplet microfluidic system for high-sensitivity multiplexed secretomic analysis on a single-cell scale (Fig. 5C).<sup>32</sup> In this setup, a single cell and smart hydrogel microparticles bound with antibodies were encapsulated within a droplet. Following incubation, specific secreted proteins from single cells were captured. The temperature-triggered shrinkage of the hydrogel immunocomplex enhances the target concentrations, facilitating sensitive multiplexed detection of the accumulated

secretions in single cells. Notably, distinct heterogeneity in low-copy-number essential secretions across six thousand cells was revealed within one hour. Nevertheless, the outcomes of this assay for secreted proteins are constrained to data at the assay endpoint, which hinders the ability to reflect the dynamic expression of the protein. In response to these challenges, Eyer *et al.* pioneered DropMap, a droplet microfluidic array technology (Fig. 5D).<sup>35</sup> This innovation facilitates the analysis of single-cell antibody secretion rates, immunoaffinity, and associated kinetic processes by immobilizing droplets on a two-dimensional array. Using DropMap, single IgG-secreting cells were encapsulated in tens of thousands of 50 pL droplets, each incorporating fluorescent markers and 300 nm paramagnetic nanoparticles. A fast and ultrasensitive in-droplet immunoassay then happened. When a magnetic field was applied, the nanoparticles captured the secreted IgG form micro aggregates that align into beadlines, allowing for the concurrent assessment of IgG secretion rates and affinities across a few thousand individual cells simultaneously. Since fluorescence-based single-cell platforms are susceptible to interference from various factors, the follow-up analysis can be compromised by the contamination. To overcome this limitation, Cong *et al.* presented a microfluidic-based surface-enhanced Raman scattering (SERS) platform for identifying cytokines secreted by individual cells.<sup>131</sup> This platform utilizes two immunological nanoprobe (a capture probe and a SERS probe) that are incorporated into the droplet containing single cells. The formation of an immunosandwich structure on the surface of cell membrane proteins captures secreted cytokines, thereby enriching them on the cell membrane surface and labeling the SERS probes for subsequent detection. This single-cell analysis platform was employed to monitor the secretion of vascular endothelial growth factor (VEGF) by specific cells from various cell lines, enabling highly sensitive detection of VEGF.

As an emerging method of protein profiling for single cells, droplet microfluidics offers several advantages: rapid encapsulation, condensed target concentration, and reduced cross-contamination. However, it suffers from low efficiency in detection due to the Poisson distribution, which results in invalid analysis caused by the presence of empty droplets or droplets containing multiple cells.

**Microwell (microengraving)-based barcoding microchips.** The microwell-based barcoding microchip is a microwell array with antibody barcoding used to quantify secreted proteins from single cells.<sup>36,132,133</sup> Love *et al.* first developed microengraving biochips, in which individual cells are captured in microwells through cell sedimentation.<sup>71</sup> The glass slides engraved with antibody arrays were covered with microwells to form single-cell sealed cavities. This setup allows for the detection of multiple secreted proteins within the cells using an immunoassay. Furthermore, Schubert and colleagues introduced a single-molecule array (SiMoA) system that enabled the determination of single-cell low-abundance proteins.<sup>134</sup> Since its inception, ongoing endeavours to enhance the sensitivity of microengraving techniques have propelled the detection of low-copy-number proteins from

single cells to the forefront of scientific inquiry. Li *et al.* introduced a novel signal amplification method depending on edge enhancement based on the vertical sidewalls of microwells for ultra-sensitive measurement.<sup>135</sup> An alternative method for enhancing fluorescence is to substitute organic dyes with quantum dots, which serve as strong readouts to lower the detection limit.<sup>136,137</sup> Besides fluorescence-based methods, Ansaryan *et al.* described a microwell array for real time spatio-temporal monitoring of secreted proteins from a few hundred single cells using a label-free nanoplasmonic imaging system.<sup>138</sup> The biosensor consists of an array of gold nanopores, which enables highly sensitive extraordinary optical transmission (EOT) spectroscopic analysis. When a secreted analyte binds to the sensor surface, it causes a change in the EOT spectra, resulting in a detectable change in intensity. However, the multiplexed detection of several secreted biomolecules simultaneously will require the implementation of functionalization methods enabling the immobilization of the corresponding receptors at spatially distinct locations on the substrate.

The detection sensitivity of conventional microwell-based methods may decrease because of the balance between the antibody bar amount and antibody density for each protein, which share the same confined space. To solve this issue, Lu and coworkers developed a new platform that combined spectral encoding and spatial encoding with microwells for the detection of secreted proteins (Fig. 5E).<sup>36</sup> This platform featured 15 isolated bars on the glass slide, each containing three different capture antibodies labeled with green, blue, and red detection antibodies separately. As a result, 42 different antibodies (except 3 positive controls) are applicable to single cell protein profiling in each microwell by the spatial location and colour signal. Specifically, 15 capture antibody bars were first fabricated on the surface of a polylysine-coated glass slide by a microfluidic DNA-encoded technology.<sup>132</sup> Secondly, single cells were loaded into microwells and the glass slide was put on the top of a microwell array for protein capture by incubation for ~20 h. Finally, the antibody barcode array slide was removed and ELISA based on 3 detection antibodies conjugated with different fluorophores was performed to readout the information of the proteins by an image analysis software. Obviously, this microwell-based method is useful and user-friendly for highly multiplexed and high-throughput detection of single-cell proteins, even dynamic detection. During the process of microwell trap and valve separation, PDMS commonly serves as the carrier material. However, studies have shown that it is not suitable for maintaining live-cell cultures. The Han group has presented a chip for single-cell culture featuring self-assembled graphene oxide quantum dots (GOQDs). This innovation facilitates high-throughput single-cell separation and maintains high activity in single-cell cultures, while guaranteeing the proper secretion and quantitative detection of multiple secreted biomarkers.<sup>139</sup> The GOQD-assembled PDMS demonstrated the highest cell activity, as evidenced by its long-term stability

and uniform size, which facilitated the highest growth rate and the largest spread area for cell culture over 72 hours. Using this method, they further presented an integrated microfluidic platform to perform multi-phenotypic profiling from exosome secretion by single cells.<sup>140</sup> This platform concurrently analyzes five phenotypic exosomes from more than 1000 individual cells, along with the secretion of inflammatory factors from the same cells.

Yang and coworkers developed a beads-on-barcode antibody microarray (BOBarray), which enables multiplexing protein detection by allocating two separate identifiers (bead size and fluorescent colour) to each protein.<sup>141</sup> Different bead sizes and colours are utilized to encode 12 different proteins. During the work, antibody-conjugated beads are incubated with the polylysine-coated glass slide to form a bead assembly featuring a barcode pattern. Each bead assembly on the glass slide can be held into 60 pL-sized microwells with a number of 15 000, leading to an increased concentration of single-cell proteins for sensitive and high-throughput analysis. Further advancement of this technique resulted in the single-cell multiplex *in situ* tagging (MIST) platform, where successive hybridization (labeling) and denaturation (quenching) of DNA-barcoded antibodies were employed for achieving ten different protein profiles (Fig. 5F).<sup>38</sup> The synergistic impact of high density DNA arrays and small microwells enabled the detection of approximately 180 protein copies from an individual cell. Based on this, they further developed a single-cell cyclic multiplexed *in situ* tagging (CycMIST) platform, enabling the analysis of a few hundred proteins within individual cells using a cocktail of UV-cleavable DNA-barcoded antibodies with high throughput and high sensitivity.<sup>142</sup>

The use of microfluidic immunoassay technology for single-cell protein profiling is a crucial component of high-throughput, multiplexed single-cell protein expression studies. It is currently the most widely used microfluidic method for single-cell protein profiling. However, this approach is significantly limited by the availability of commercial antibodies and cannot analyze antibody-deficient protein targets. Additionally, immunological analysis methods relying on antigen-antibody interactions face challenges related to cell permeability, molecular crowding, epitope accessibility, and cross-reactivity, all of which considerably hinder throughput and accuracy.

### Non-antibody-based protein profiling strategies

While antibody-based assays dominate current microfluidic single-cell protein profiling platforms, an expanding set of non-antibody (or antibody-independent) recognition strategies is emerging to complement conventional immunoassays. Aptamer-based reagents provide chemically defined binders with favorable stability and engineering flexibility. For example, fluorescent-quenching aptamer-based single-cell western blotting (FAS-WB) enables multiplex single-cell protein detection by using fluorophore-labeled aptamers together with complementary quenching strands, thereby reducing the

substantial signal loss typically associated with repeated antibody stripping in scWestern workflows.<sup>143</sup> Beyond gel-based formats, aptamers can also be coupled to sequencing readouts to achieve scalable multiplexing; notably, Apt-seq leverages the inherent “sequence-ability” of aptamers to support high-throughput multiplex quantification at single-cell resolution and can be extended toward multimodal measurements.<sup>144</sup>

In parallel, phage-display-based strategies offer an alternative route to translate protein binding into sequencing-compatible barcodes. PHAGE-ATAC integrates nanobody-displaying phages with droplet-based single-cell ATAC-seq to jointly profile surface protein signals and chromatin accessibility, enabling multimodal single-cell analysis.<sup>145</sup> Phage-based barcoding has also been applied to rare-cell scenarios: nanoparticle-directed capture combined with phage barcodes and next-generation sequencing enables efficient enrichment and multiplex profiling of rare single cells on integrated microfluidic chips.<sup>146</sup> Finally, non-antibody recognition strategies can be interfaced with orthogonal analytical modalities; for instance, a microfluidic flow cytometry-mass spectrometry ( $\mu$ CytoMS) workflow has been developed to quantify drug uptake and associated protein-expression changes at the single-cell level, while minimizing sample loss introduced by centrifugation.<sup>147</sup>

### Microfluidic mass spectrometry

MS-based proteomics allows for large-scale proteome compositional, structural and dynamic changes to be resolved in a label-free manner. It has been widely used to characterise proteins, post-translational modifications and proteoform dynamics, enabling comprehensive and in-depth connection and molecular pathways of proteins to biological processes or disease progresses.<sup>148</sup> Ongoing improvements in the detection sensitivity of MS have driven substantial progress, making it possible to analyze low-abundance proteins in a wide variety of clinical specimens, such as rare cell samples and formalin-fixed paraffin-embedded (FFPE) samples.<sup>149,150</sup> However, single-cell proteomics using MS has been mainly impeded due to the lack of miniaturized sample handling techniques and effective separation methods.<sup>3,151–153</sup> The recent integration of microfluidic sample preparation techniques with mass spectrometry, along with advancements in the instrumentation, has enabled the measurement of proteins at the single-cell level.<sup>154</sup> For instance, highly miniaturized and automated microfluidic sample preparation systems based on picoliter-scale microwells have been developed to confine single cells, accelerate on-chip digestion, and streamline peptide extraction for single-cell MS-based multi-omics analysis.<sup>155</sup> Recent advances in MS-based single-cell proteomics have been driven by jointly optimized low-loss sample handling and next-generation instrumentation, enabling substantially deeper proteome coverage and improved scalability. For example, the Chip-Tip workflow demonstrated deep label-free single-cell proteomics with enhanced sensitivity and

throughput,<sup>156</sup> and systematic evaluation on the Orbitrap Astral platform further clarified acquisition and quantification considerations for low-input and single-cell measurements.<sup>157</sup> The following section will focus on a system for single-cell proteome analysis that combines microfluidics with MS.

**Valve-based microfluidic mass spectrometry.** To explore the usefulness of valve-based microfluidics coupled with MS, Alexandra Ros and coworkers developed a microfluidic MS approach for single-cell protein analysis.<sup>158</sup> The entire workflow for cell analysis, encompassing cell lysis, protein capture, digestion, and deposition of the matrix-assisted laser desorption ionization (MALDI) matrix, was seamlessly integrated onto a microfluidic chip before subsequent MALDI-time-of-flight (TOF) detection. A reversible attachment method between an ITO substrate and PDMS manifold was used, enabling the removal of PDMS to expose matrix crystals on the ITO substrate for MALDI-TOF analysis. This approach was utilized for assessing the number of Bcl-2 in MCF-7 cells. The sensitivity of this method reached the detection of high abundant proteins in single cells and quantitative protein characterization in small cell ensembles.<sup>159,160</sup> Furthermore, Gebreyesus and coworkers presented a streamlined workflow that integrates microfluidic chips for comprehensive proteomic sample preparation with data-independent acquisition (DIA) MS for single-cell proteomic analysis (Fig. 6A).<sup>3</sup> Essentially, the structure of the microfluidic chip includes a chamber for cell capture, a vessel for protein digestion, and a C18 beads-packed column for desalting. The cell chambers consisted of wedge-shaped pairs of pillars to separate defined numbers of cells. After trapping, the cells were subjected to successive treatments, including cell lysis, protein digestion, and desalting, which ultimately resulted in the cleanup of peptides. The integrated workflow streamlined multiplexed and automated cell isolation, counting, imaging and sample processing in a single device, enabling the profiling of  $\sim$ 1500 protein groups across 20 single mammalian cells. However, the resulting peptides still needed to be extracted for subsequent analysis by liquid chromatography-tandem mass spectrometry (LC-MS/MS). To improve robustness and throughput, dedicated sample-preparation hardware has been developed to better interface with standardized LC-MS workflows. The proteoCHIP EVO 96 was introduced as a sample preparation chip that directly interfaces with the Evosep One, aiming to enhance reproducibility and throughput for sensitive low-input and single-cell proteomics.<sup>161</sup> Additionally, continuous flow microfluidic systems based on multi-pumps/valves control are susceptible to throughput issues, which need to be considered for practical applications.

**Droplet microfluidic mass spectrometry.** Droplet microfluidics combined with MS have proven to be exceptional tools, enabling high-throughput sample preparation for single-cell proteomics. Li *et al.* reported a self-aligned monolithic device combining droplet microfluidic device and shotgun proteomic analysis techniques for single cell proteomic analysis

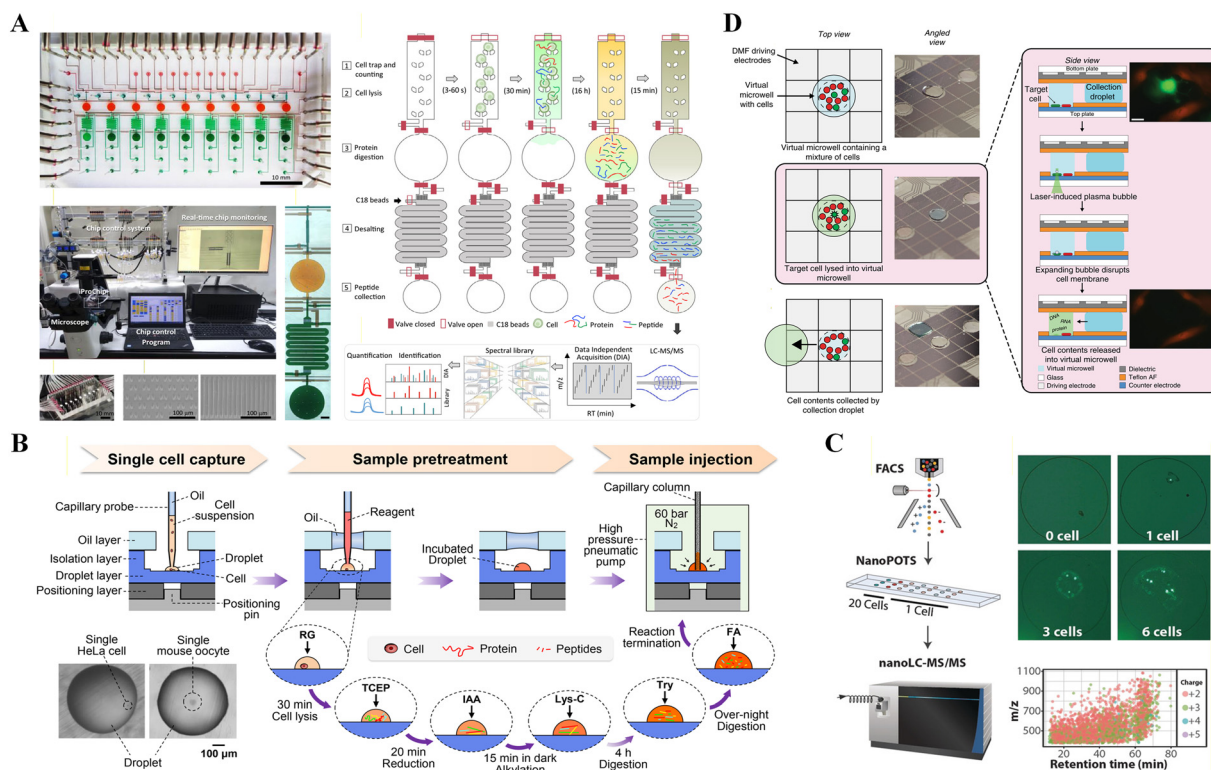


**Fig. 6** Microfluidic mass spectrometry for single-cell protein analysis. (A) Schematics of the integrated proteomics chip and streamlined workflow for nanoproteomics. Reproduced with permission.<sup>3</sup> Copyright 2022, Springer Nature. (B) Schematics of the setup of the nanoliter scale oil-air-droplet (OAD) chip to conduct multistep complex sample pretreatment for LC-MS/MS shotgun proteomic analysis. Reproduced with permission.<sup>16</sup> Copyright 2018, the American Society Chemistry. (C) Workflow of single cell proteomic analysis in the nanoPOTS chip by nanoLC-MS/MS. Reproduced with permission.<sup>19,20</sup> Copyright 2018, Wiley-VCH Verlag. (D) Illustration of the platform used for DISCO: a single cell is targeted for laser lysis into the collection droplet. The collection droplet is queued for proteomic analysis. Reproduced with permission.<sup>26</sup> Copyright 2020, Springer Nature.

(Fig. 6B).<sup>16</sup> The design featured an on-chip oil-air-droplet (OAD) structure for performing sample processing. It can decrease the sample loss by minimizing adsorption on the reactor surface and sample transfer. In addition, a nanoliter reaction volume was employed to further reduce the droplet contact area on the chip. The system was employed to detect 51 and 335 protein species, respectively, from a single HeLa cell and a mouse oocyte. The performance was additionally improved through the incorporation of nanoLC, as demonstrated by leading research teams.<sup>162</sup> The technique features a significantly faster separation, a much smaller injection volume, and a higher separation efficiency. For example, Zhu *et al.* presented a robotically addressed chip-based nanodroplet processing platform using nanoLC-MS, termed nanoPOTS (nanodroplet processing in one pot for trace samples), which can realize ultra-sensitive proteomic analysis for single mammalian cells.<sup>19,20</sup> The platform demonstrated reproducible and quantitative proteomic measurements, where ~670 protein groups were recognized from single HeLa cells (Fig. 6C). In addition, parallelized preparation strategies can improve throughput without relying on sophisticated robotic liquid handling. A parallel sample-processing workflow has been reported to simultaneously process multiple single cells

for scMS, illustrating a practical route to scaling sample preparation.<sup>163</sup> Recently, an update edition of nanoPOTS, nested nanoPOTS (N2), has achieved additional miniaturization of the sample processing volume, decreasing it from 200 nL to 30 nL, and integrated isobaric labeling workflows.<sup>164</sup> Massively parallel preparation has also been enabled by nanoliter-scale droplet processing on open substrates. The nPOP protocol describes parallel preparation of thousands of single cells in nanoliter droplets on glass slides and emphasizes flexibility for different multiplexed MS strategies, providing a practical route for scalable single-cell proteomics sample preparation.<sup>165</sup> These enhancements have increased throughput, allowing for the analysis of 27 to 1827 samples per assay with improved detection sensitivity.

**Digital microfluidic mass spectrometry.** The DMF device is an electric field-based microfluidic technique that is used to perform single-cell protein profiling by discrete droplet operation in a flexible, addressable, and contactless manner. The Wheeler group has performed a range of groundbreaking research studies on DMF platforms for cell assays,<sup>166</sup> sample preparation for MS,<sup>167-169</sup> and proteomics.<sup>170</sup> Following this, an on-chip sample clean-up step was performed by solid-phase extraction on porous polymer monoliths.<sup>170</sup> Based on

these previous fundamental works, Leipert *et al.* constructed the first DMF platform for cellular proteomics using MS.<sup>171</sup> They introduced the single-pot, solid-phase-enhanced sample preparation (SP3) approach, enabling the removal of salts and anti-fouling polymeric detergents. This advancement made sample preparation *via* DMF compatible with LC-MS-based proteome analysis. Utilizing DMF-SP3 for proteome analysis of Jurkat T cells resulted in the identification of up to 1200 proteins from around 100 cells using Orbitrap MS. They further improved the sensitivity of DMF-SP3 using a high-field asymmetric-waveform ion mobility spectrometry (FAIMS) and ion fractionation to identify around 5000 proteins from single nematodes.<sup>172</sup> Along with isobaric labeling, a recent extension of DMF-SP3 has shown an average of 1815 protein groups from 75 Jurkat T cells.<sup>173</sup> Beyond individual processing steps, end-to-end digital microfluidics has also been demonstrated for proteomics sample preparation. An All-in-One DMF pipeline was reported to integrate reduction, alkylation, digestion and isotopic labelling within a single automated DMF workflow, highlighting the potential of DMF for low-loss, contamination-minimized processing of mass-limited samples.<sup>174</sup> Furthermore, the DISCO platform was utilized to perform single-cell proteome analysis combined with nanoLC-MS/MS (Fig. 6D).<sup>26</sup> In DISCO, a focused, high-energy laser is used to lyse the target cells within a few micrometers of the focal point. Aliquots of cell lysate collected from DISCO devices were subjected to the proteomic pipelines. This approach identified an average of 427 proteins from a single cell. The numbers of detected proteins are comparable to those reported in single-cell proteomics studies in the absence of the peptide desalting step. The system can be subjected to full integration of online single-cell proteomic pipelines on a DMF chip in the future to improve protein detection sensitivity. More recently, Yang and coworkers presented an integrated sample processing on an active-matrix digital microfluidic chip for single-cell proteomics (AM-DMF-SCP).<sup>175</sup> By employing an active matrix backplane to replace traditional electrodes, this approach overcomes the limitations of electrode size and number on previous DMF chips. The reduction of the electrode size significantly decreased the sample loss of proteins in single cells, and the increase of the number of electrodes substantially enhanced the throughput of single-cell sample processing on a digital microfluidic chip. Utilizing the AM-DMF-SCP approach in conjunction with data-independent acquisition (DIA), the system is capable of identifying an average of 2258 protein groups in single HeLa cells within 15 minutes of the LC gradient.

### Microfluidic sequencing

Although MS can perform large-scale single-cell proteome analysis, it is difficult to achieve the direct and accurate quantification of plentiful proteins of single cells. TMT (tandem mass tag),<sup>176</sup> LFQ (label free quantification),<sup>177</sup> and

DIA<sup>178</sup> are three MS-based high-throughput proteomics quantification methods that have been developed to date, of which TMT is the most commonly used. TMT using metal isotope tags in mass cytometry can detect ~100 of proteins quantitatively. However, this method was also limited by isotopic impurities, signal sensitivity and difficult sample operation.<sup>179,180</sup> Therefore, there is a need for a large-scale quantitative proteome assay strategy for single cells.<sup>181</sup> As an alternative, short DNA sequences, known as DNA barcodes, have been recommended as highly effective signature tags.<sup>182</sup> An 8 bp DNA sequence alone can generate 65 536 unique sequences, providing sufficient tags for a wide array of proteins of interest. The Abate group first developed a method called Ab-seq, which used DNA-barcoded antibodies to stain single cells, that allowed proteins to be profiled with droplet microfluidic barcoding and DNA sequencing.<sup>2</sup> In this way, the amount of the antigen epitope can be inferred based on the amount of the DNA barcodes (Fig. 7A). This method is highly sensitive and multiplexing, achieving efficient sequence amplification and numerous DNA signature tags. Recently, Cai *et al.* proposed an automated split-pool barcoding method based on digital microfluidics to perform high-throughput and high-integration single-cell protein analysis.<sup>11</sup> The cells are successively incubated with the mixed DNA-tagged antibody panels and magnetic beads off chip, for protein encoding and cell manipulation, respectively (Fig. 7B). The tagged DNA includes three parts: an antibody barcode for protein encoding, a universal primer for DNA amplification, and a poly(A) sequence for subsequent ligation reaction. The split and pool process is initiated by evenly dividing up the cells and loading them into the reservoir of the DMF chip at a concentration of 10–200 cells per reservoir. By repeating the split and pool approach, the DNA-tagged antibodies in each cell share the same cell-specific barcode consisting of four subcodes since all the objects in a cell travel through the same random synthesis path during each of the splits. The cell throughput can be expanded by adding the number of reaction reservoirs or ligation rounds. The protein expression matrix is finally obtained by identifying the antibody barcode, cell barcode and UMIs. In DMF-Protein-seq, a high mapping rate and recovery level of cell barcode is ensured by the low loss of cells, successful ligation of subcodes, and efficient removal of the free subcodes in the last round.

While many sequencing-assisted protein profiling strategies rely on antibody-derived tags, emerging non-antibody approaches—such as aptamer-based barcoding (*e.g.*, Apt-seq) and phage-based protein indexing (*e.g.*, PHAGE-ATAC) have demonstrated that sequencing readouts can also be achieved using alternative affinity reagents.<sup>144,145</sup>

### Microfluidic single-cell multi-omics

Regulating individual cells is a complex process involving various classes of molecules, including DNA, RNA, proteins, and small molecules. Profiling cells in just one dimension

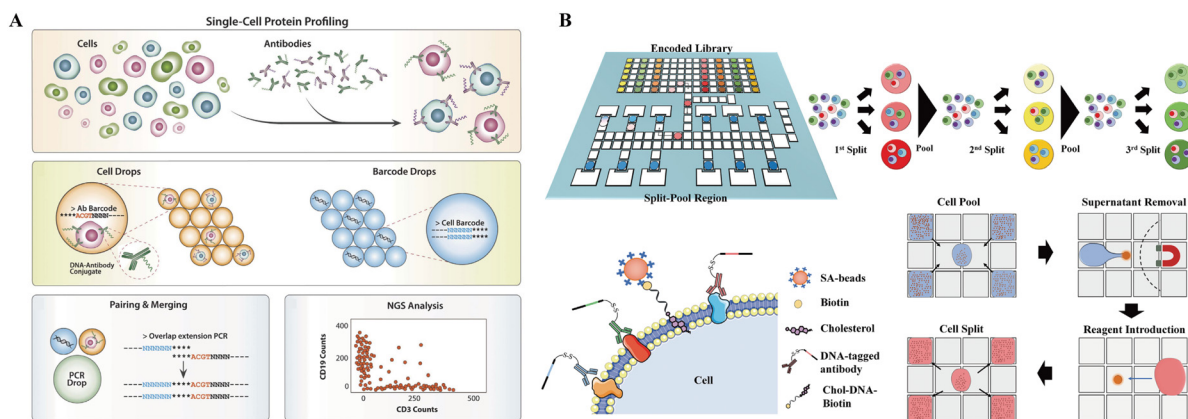


**Fig. 7** Microfluidic sequencing for single-cell protein analysis. (A) The workflow of Ab-seq: cells are stained with antibodies labeled with unique sequence tags. To read out single cell protein expression, a microfluidic workflow conjugates the antibody tag sequences bound to the cell with unique cell barcode sequences. Reproduced with permission.<sup>2</sup> Copyright 2017, Springer Nature. (B) Schematic of DMF-Protein-seq: leverages split and pool strategy on DMF chip, allowing for simultaneously tagging and sequencing thousands of single cells in one experiment. Reproduced with permission.<sup>11,12</sup> Copyright 2024, Wiley-VCH Verlag.

fails to offer a complete view. Additionally, discrepancies have been observed between the genome, transcriptome, and proteome correlations. Joint profiling of multiple datasets allows for identifying causal regulatory relationships and enhances the resolution of single-cell atlases. Microfluidic-assisted single-cell multi-omics analysis facilitates the separation, extraction, and identification of different cellular components in a high-throughput, cost-effective, and straightforward manner.

**Simultaneous quantitation of mRNA and proteins in single cells.** Simultaneous detection of the protein profiling and transcriptome in individual cells offers a comprehensive view of expression and phenotypic dynamics, while establishing the correlation between RNA and protein functional networks.<sup>183–185</sup> The SCBC chip combined with bead-based transcriptomics was firstly designed to measure intracellular proteins and transcripts from single cells.<sup>186</sup> In detail, they combined bead-based transcriptomics with SCBC to measure intracellular proteins and transcripts from single cells. Transcripts and proteins are measured independently using sequencing and fluorescent immunoassays, respectively, to maintain their optimal measurement conditions. These measurements are then correlated by encoding the physical locations of the cells into a digital sequencing space through the use of spatially patterned DNA barcodes (Fig. 8A). Based on this method, the Yang team presented a multi-paired-seq microfluidic platform to further improve cell utilization.<sup>5</sup> Following incubation with antibody–DNA barcodes, the cells were loaded directly into the chip, resulting in high-performance cell trapping and cell-barcode bead pairing based on the principles of hydrodynamics. Precise fluidic manipulation realized by multi-pump/valve control enables comprehensive mixing and washing, thereby markedly enhancing the sensitivity of transcriptomic and proteomic analysis. To facilitate high-throughput integrative analysis of transcriptomes and cell surface proteins in individual cells, techniques combining

droplet microfluidics with single-cell RNA sequencing (scRNA-seq) have been established. Utilizing the technology of antibodies conjugated to DNA barcodes, two different research teams developed similar works by combination with Drop-seq technology,<sup>187</sup> called REAP-seq<sup>188</sup> and CITE-seq,<sup>189</sup> respectively, for the simultaneous determination of proteins and mRNA in single cells (Fig. 8B).<sup>15</sup> In these strategies, DNA-tagged antibodies are utilized to specifically encode cell surface proteins. The DNA tag includes an amplification handle, an antibody barcode, and a poly(A) tail. The DNA-tagged antibody library is firstly used to incubate the cells, followed by a procedure similar with Drop-seq. This enables the capture of both mRNA and DNA-labeled antibodies from individual cells on barcoded beads within a single droplet. Subsequently, sequencing is performed to determine the type and quantity of mRNA and surface-bound antibodies in the same cell, allowing for high-throughput quantification of both mRNA and protein. Integration of this approach with droplet-based microfluidics provides strong potential for high-dimensional single-cell protein profiling. It enables the simultaneous acquisition of multiple layers of cellular information, including proteomic and transcriptomic data, within individual cells. Additionally, using unique UMIs for each protein counting can eliminate the amplification bias and obtain the exact data of protein expression. By applying the antibody barcoding approach to 5' capture-based single-cell RNA sequencing methods, ECCITE-seq enables high-throughput analysis of six distinct information modalities from each individual cell. These modalities include transcriptome, T-cell receptor, surface protein, sample identity by hashtags, and sgRNA.<sup>190</sup> Furthermore, Mimitou *et al.* presented an assay for transposase accessible chromatin (ATAC) with select antigen profiling by sequencing (ASAP-seq), enabling the combination of CITE-seq for profiling epigenomic, transcriptomic and proteomic changes after T cell stimulation.<sup>191</sup> The ASAP-seq workflow is fully compatible with related multimodal assays that concurrently measure

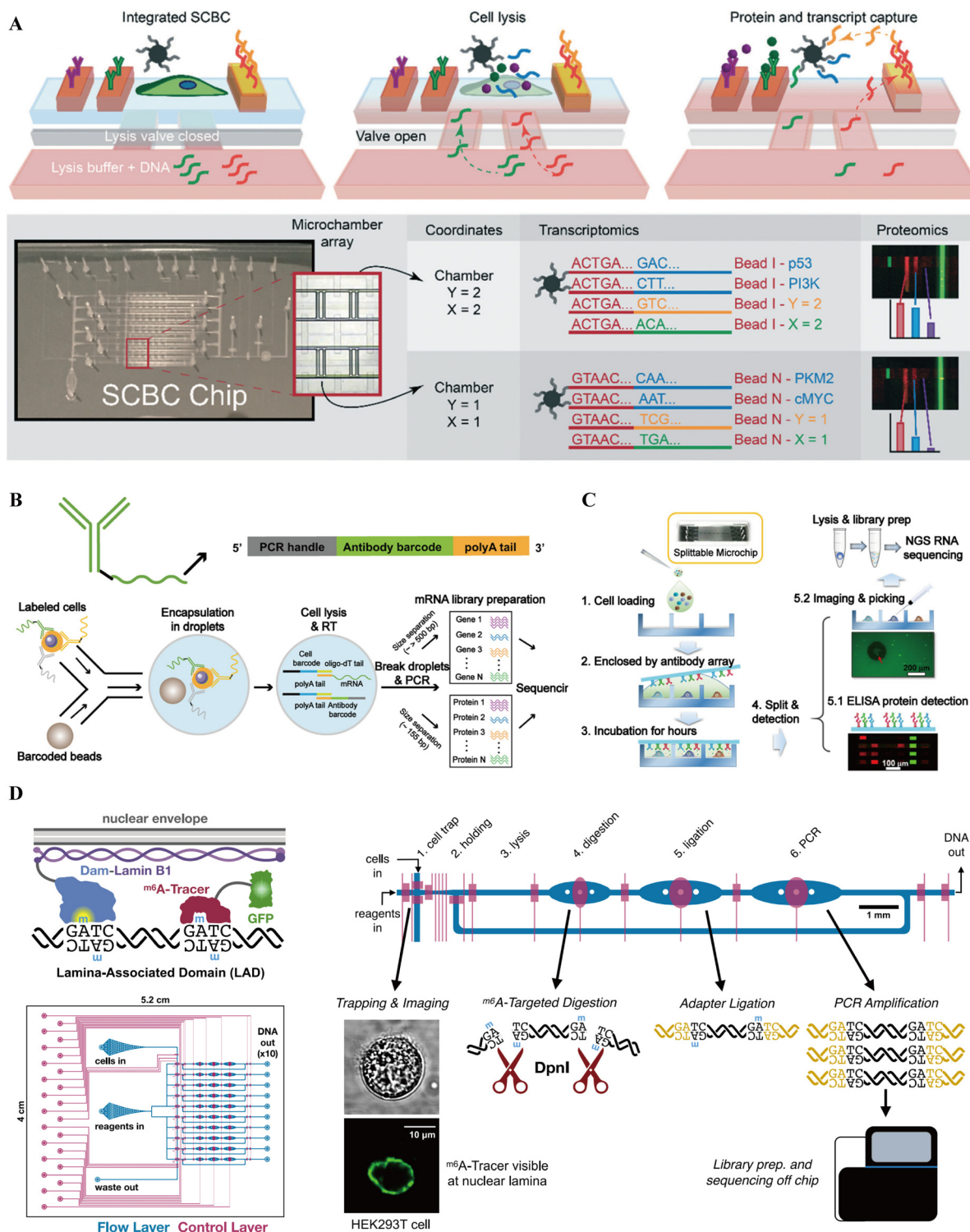


**Fig. 8** Microfluidic single-cell multi-omics. (A) Schematic workflow of the multi-omic SCBC built on the SCBC microfluidic platform. Reproduced with permission.<sup>5</sup> Copyright 2018, The Royal Society of Chemistry. (B) Schematic of REAP-seq and CITE-seq with antibody–DNA barcode-labeled cells processed by Drop-seq. Reproduced with permission.<sup>12,15</sup> Copyright 2023, Elsevier. (C) Schematic of a splittable microfluidic chip for capturing single cells, along with their secreted proteins. Reproduced with permission.<sup>12,18</sup> Copyright 2016, the American Chemical Society. (D)  $\mu$ DamID device design and function: 10-cell device showing the DamID protocol and the function of each chamber of the device to perform cell trapping, imaging, and processed in parallel. Reproduced with permission.<sup>24</sup> Copyright 2020, Elsevier.

protein and RNA. Notably, the introduction of a bridge oligo facilitates the utilization of existing antibody conjugates,

offering an accessible and user-friendly protocol. Lately, Swanson and coworkers presented the TEA-seq method to

measure mRNA, epitopes, and chromatin accessibility of single cells at the same time in a high-throughput manner.<sup>192</sup> Different from the co-assay of proteins and mRNA in each individual cell, the strategy of sample splitting for mRNA and secreted cytokine proteins in the same single cells was developed (Fig. 8C).<sup>18</sup> Single cells were dispensed into individual wells for culture, where multiplexed antibodies on a sealed slide were utilized to capture the secreted proteins. The secreted proteins were then characterized using fluorescence imaging and ELISA, which is similar to the protocol of microwell-based barcoding microchips. Subsequently, cells secreting specific proteins were selected for scRNA-seq. This strategy identified a subgroup of genes that were highly coexpressed and correlated with TNF- $\alpha$  secretion in mouse macrophage cells. An analogous approach was applied to quantify immune dynamics in individual cells.<sup>193</sup> However, this strategy of sample splitting exhibited relatively low sensitivity and limited throughput when measuring proteins.

The interaction between proteins and DNA is of great importance in the regulation of gene expression. However, the manner in which the cell heterogeneity of protein–DNA binding affects the variability of gene expression remains unclear. scDam and T-seq, single-cell DNA adenine methyltransferase identification with mRNA sequencing of the same cell, was introduced for the simultaneous quantification of protein–DNA interaction and gene expression.<sup>194</sup> Based on this, Altomose and coworkers presented a  $\mu$ DamID technique within an integrated microfluidic framework, enabling concurrent imaging and sequencing of protein–DNA interactions in individual cells.<sup>195</sup> As shown in Fig. 8D, the platform enables single-cell isolation, imaging, and sorting, followed by DamID in a microfluidic chip.<sup>24</sup> The paired imaging data from single human cells were improved using an improved m6A-Tracer protein. They validated interactions between DNA and proteins found at the nuclear lamina, and observed variable 3D chromatin organization and broad gene regulation patterns.  $\mu$ DamID offers a distinctive capability for analyzing paired imaging and sequencing data at both the single-cell level and across different cells, facilitating the integrated examination of nuclear localization, sequence identity, and the variability of protein–DNA interactions.

While joint measurements of RNA and protein expression have been achieved, suitable methods for visualizing combined transcript–protein datasets to characterize differences in expression abundance and dynamic range remain lacking. Additionally, it is still challenging to detect specific transcripts and proteins of interest that are below the limit of detection.<sup>196</sup> Given recent advancements in microfluidics and its deeper integration into spatiotemporal genomics, there is a strong rationale to believe these challenges will be addressed in the future.

**Simultaneous quantitation of metabolites and proteins in single cells.** Compared to other single-cell ‘-omics’ approaches, metabolomics offers a more immediate and dynamic representation of cellular functionality in single cells.<sup>39</sup>

Nevertheless, measuring the metabolome at the single-cell level poses a significant challenge owing to the rapid dynamics of metabolism, which can shift within seconds. Additionally, performing comprehensive metabolome analyses is difficult because of the large number of metabolites and their substantial concentration variations. Microfluidic chips, with their controllability, rapid response times, and high-throughput capabilities, offer an ideal solution to these challenges. The Heath team presented chemical approaches for integrated metabolic and proteinic experiments from single cells.<sup>197</sup> Fluorescence quantification for intracellular metabolites and proteins were performed by surface-competitive binding assays and immunoassays with fluorescence reporters. The SCBC was used to investigate how human-derived glioblastoma cancer cells respond to epidermal growth factor receptor inhibition. This study represented a report detailing both intercellular metabolic heterogeneity and alterations in the metabolite–phosphoprotein correlation network in response to drug treatment. The platform enables the simultaneous and highly accurate measurement of variation in metabolism and the interactions between metabolites and signaling proteins for the first time. Subsequently, they additionally developed a supramolecular surface competition assay to screen glutamine analogs and uncovered novel interactions between phosphoprotein signaling and cellular energy pathways.<sup>198</sup> In this system, Cy3-labeled cyclodextrins fixed onto glass surfaces act as supramolecular hosts, while adamantane-BHQ2 conjugates serve as guests. This arrangement integrated a SCBC system with a multiplexed panel of 15 additional metabolites, along with associated metabolic enzymes and phosphoproteins for fluorescence detection. High glucose uptake and activation of oncogenic signaling pathways are hallmark characteristics of cancer cells. These traits, along with the mutational spectrum, have become key indicators for the diagnosis for CTCs. Due to the extensive heterogeneity of CTCs, it is crucial to analyze signals and their correlations at single-cell resolution to avoid obscuring important correlations that might be hidden in data obtained from cell population-based approaches.

## From biology to the clinic

Beyond methodological innovation, single-cell protein profiling contributes uniquely to biological research and clinical applications by directly measuring functional phenotypes—such as receptor abundance, post-translational modifications, and secretion—that are not directly accessible from single-cell RNA sequencing (scRNA-seq). The following sections summarize how these protein-layer readouts complement transcriptomics and enable more actionable interpretations in immunity, cancer, and clinical translation.

### Beyond scRNA-seq

ScRNA-seq has transformed our ability to define cell types and transcriptional programs. However, transcript abundance alone is often insufficient to infer protein abundance or cellular function because gene expression is shaped by

extensive post-transcriptional regulation, context-dependent translation, and protein turnover.<sup>199,200</sup> As a result, key aspects of cellular behaviour cannot be directly inferred from transcriptomic data alone.

Proteins are the primary executors of biological function and the direct mediators of signalling, cell–cell communication, and therapeutic response. Critical functional features—including post-translational modifications, receptor activation, enzymatic activity, and protein secretion—are largely invisible to RNA-based measurements.<sup>201</sup> For example, REAP-seq explicitly motivates joint RNA–protein measurement by noting that protein abundance cannot necessarily be inferred from mRNA abundance and that an unbiased view of proteins is necessary to model cellular responses.<sup>202</sup> Single-cell protein profiling therefore provides a functionally grounded layer of information that is orthogonal to transcriptomics, enabling more direct interpretation of cellular states and phenotypes. Recent work integrating single-cell proteomic and transcriptomic data has underscored the value of joint analysis. Such integration reveals cellular diversity and functional phenotypes that would be obscured when using RNA data alone.<sup>203</sup> These findings demonstrate that protein-level measurements provide orthogonal and complementary information to scRNA-seq.

### Functional profiling of signalling and immunity

A major advantage of single-cell protein profiling is its ability to capture functional phenotypes that are difficult to infer from transcript abundance alone. In many contexts, cellular decisions are governed by rapid and reversible changes in protein activity—such as receptor engagement, conformational changes, and post-translational modifications—that precede or occur independently of transcriptional remodelling. Accordingly, protein-level measurements provide a proximal readout of pathway engagement and state transitions, improving the interpretability of heterogeneous responses to environmental cues or perturbations.

Signalling-state profiling is a representative example. Multiplexed measurements of intracellular proteins enable direct interrogation of pathway activation and drug-target modulation at single-cell resolution, thereby resolving heterogeneous signalling responses that are often obscured in population-averaged assays. Importantly, signalling-state profiling can refine cell-state annotations beyond static markers, distinguish transient activation from stable lineage identity, and support mechanism-of-action studies during perturbations. Mass cytometry primers and methodological overviews further detail how multiplexed panels can interrogate signalling networks and functional programs at scale. Bendall *et al.* demonstrated single-cell mass cytometry as a platform for multiplexed measurement of immune signalling behaviours and differential drug responses across hematopoietic cell subsets.<sup>204</sup> Complementary to mass cytometry, phospho-flow cytometry provides practical, clinically oriented assays for quantifying pathway activation, and has been increasingly discussed in the context of diagnostic development and validation.<sup>205</sup>

In parallel, immune systems highlight why protein profiling is often indispensable: functional outputs frequently determine biological consequence. For instance, cytokine secretion, cytotoxic effector release, and ligand–receptor interactions are core determinants of immune activity, yet they may not be faithfully represented by mRNA levels at a single time point. Microfluidic single-cell protein assays provide a direct route to quantify these behaviours by isolating individual immune cells and measuring secreted or surface-associated proteins over defined time windows. Microengraving, originally introduced as a soft-lithographic microwell-array approach, enables high-throughput mapping of proteins secreted by individual viable cells and supports the rapid identification of functional immune subsets.<sup>206</sup> Subsequent quantitative implementations demonstrated that secretion rates and frequencies of multiple cytokines can be measured at single-cell resolution, enabling a more mechanistic dissection of immune response heterogeneity than bulk assays.<sup>207</sup>

Taken together, functional profiling of signalling and immune outputs provides a practical framework for connecting cellular states to actionable phenotypes. By combining controlled microenvironments with multiplexed protein readouts, microfluidic single-cell assays can reveal how signalling engagement translates into immune effector function, thereby offering a mechanistically grounded complement to transcript-centric analyses in immunology, inflammation, and therapeutic response studies. In cancer immunology, single-cell technologies have been instrumental in defining operational principles of T cell dysfunction and response to checkpoint blockade, motivating functional profiling as a complement to transcriptional readouts.<sup>208</sup>

### Cancer and biomarkers

Cancer is characterized by profound intratumoral heterogeneity and microenvironmental complexity, making protein-level single-cell profiling highly relevant for biomarker discovery and translational stratification. Many clinically deployed biomarkers are protein-based, with established assays and interpretive criteria. For example, HER2 assessment in breast cancer is guided by professional recommendations and scoring frameworks that rely heavily on immunohistochemistry and ISH interpretation. Likewise, PD-L1 testing has formalized roles as an FDA-reviewed companion diagnostic in multiple indications, underscoring that clinically actionable decisions can depend directly on protein quantification and scoring thresholds.

Single-cell protein profiling adds value by revealing cell-to-cell variability in marker expression (including heterogeneous or spatially restricted biomarker patterns), identifying resistant subpopulations, and clarifying tumour–immune interactions that may not be apparent from bulk assays. Spatially resolved protein technologies further strengthen this link to clinical pathology. For example, three-dimensional imaging mass cytometry enables multiplexed tissue mapping

at single-cell resolution and was demonstrated in human breast cancer specimens to resolve microenvironmental organization not accessible in 2D alone.<sup>209</sup> At a broader landscape level, recent perspectives have emphasized how proteomics is progressing “from single cells to clinical applications”, including connections to spatial profiling and translational workflows.<sup>210</sup>

### Clinical translation and standardization

For single-cell protein profiling to the transition from exploratory research to clinical application, standardization and validation across the entire workflow are essential. Unlike transcriptomic assays, which are primarily research-oriented, many protein-based measurements already underpin routine clinical diagnostics, providing a clear translational precedent. However, microfluidic single-cell protein assays introduce additional variables that must be systematically addressed before clinical adoption.

A critical consideration is controlling pre-analytical variables, including sample collection, handling, processing time, and fixation or permeabilization strategies, all of which can substantially influence protein integrity and quantitative readouts. Analytical validation should be fit-for-purpose but typically encompasses precision, sensitivity or limit of detection, robustness, and stability, with additional attention to single-cell-specific factors such as cell recovery, rare-event detection, and segmentation or gating uncertainty. Established regulatory principles for bioanalytical method validation can provide useful guidance for structuring performance claims and documentation, even though single-cell assays may require tailored evaluation criteria.

Clinical flow cytometry offers a valuable reference framework for translation. Standardized validation guidelines and reporting requirements developed for flow cytometry illustrate how multiplexed single-cell protein assays can achieve reproducibility, inter-laboratory comparability, and regulatory acceptance. CLSI H62 outlines validation strategies and instrument standardization for cell-based assays, and MIFlowCyt defines the minimum reporting information to support reproducibility and inter-study comparability.<sup>211</sup>

These principles are directly relevant to emerging microfluidic platforms, particularly as they increasingly incorporate automation, standardized reagents, and closed or cartridge-based workflows to reduce operator-dependent variability.<sup>212</sup>

From a practical perspective, pathways toward clinical adoption are likely to prioritize targeted, clinically actionable protein panels rather than discovery-scale measurements, along with harmonized data analysis and reporting pipelines. Early alignment with quality-management systems and regulatory expectations can further facilitate downstream implementation.<sup>213</sup> Collectively, these considerations highlight that the clinical value of single-cell protein profiling lies not only in technological innovation, but also in its ability to deliver robust, interpretable, and functionally meaningful protein-level information that complements transcriptomic approaches and supports diagnostic and translational decision-making.

### Conclusion and outlook

In contrast to the rapid advancement of single-cell sequencing technology, the development of protein profiling in single cells has lagged behind over an extended period. The primary reason for this is the complexity of proteomic sample processing, the low protein abundance, and the scarcity of protein labelling and amplification techniques.<sup>214</sup> Microfluidics-based systems have the advantages of an integrated and automated operation, high efficiency and accuracy, low cost and miniaturization, which stimulate the advances of single-cell protein profiling towards high-throughput and multimodal dimensions using microfluidic devices. This review offers a succinct summary of how microfluidics has advanced the development of protein profiling for single-cell analysis: single-cell separation strategies include trap, valve, droplet, well and field-based methods, facilitating the simultaneous processing of tens of thousands of cells within a single sample; integrated microfluidic single-cell microreaction systems and modular micro–nano interfaces facilitate straightforward coupling with output equipment; microfluidic platforms for rapid and high-throughput single-cell protein tagging facilitate the generation of large-scale quantitative molecular datasets, dramatically enhancing the

**Table 1** Overview of typical microfluidic single-cell protein profiling methods

Analytical tool	Target	Microfluidics	Technique	Multiplexity	Throughput	Sensitivity	Workflow steps	Ref.
CE	Known	Valve	CE-LIF	~10	~1–10 cells	~0.1 pM	7	22
		Well		~10	~1–10 cells	~0.1 pM	7	95
WB		Well	scWestern	~10	~10 <sup>3</sup> –10 <sup>4</sup> cells	Antibody-limited	6	27
FCM		Valve	MicroFC	~30	~10 <sup>3</sup> –10 <sup>4</sup> cells	Antibody-limited	4	4
		Droplet	FDC	~30	~10–10 <sup>2</sup> cells	~10 <sup>2</sup> –10 <sup>3</sup> copies	5	23
Immunoassay		Valve	SCBC	~40	~10 <sup>3</sup> –10 <sup>4</sup> cells	~10 <sup>2</sup> –10 <sup>3</sup> copies	5	21
		Droplet	DropMap	~10	~10 <sup>4</sup> –10 <sup>5</sup> cells	~500 copies	6	35
		Well	Microengraving/MIST	~40	~10 <sup>3</sup> –10 <sup>4</sup> cells	~10 <sup>2</sup> –10 <sup>3</sup> copies	5	36, 38
MS	Unknown	Valve	SciProChip	~1500	~1–5 cells	~10 <sup>6</sup> copies	6	158
		Droplet	OAD/nanoPOTS	~1000	~10–10 <sup>2</sup> cells	~10 <sup>4</sup> –10 <sup>5</sup> copies	7	16, 19, 20
		Field	AM-DMF-seq	~2000	~20–60 cells	~10 <sup>4</sup> –10 <sup>5</sup> copies	6	175
Sequencing	Known	Droplet	Ab-seq	Unlimited	~10 <sup>4</sup> cells	Antibody-limited	5	2
		Field	DMF-Protein-seq	Unlimited	~20–60 cells	~10 <sup>4</sup> –10 <sup>5</sup> copies	6	11

detection of a broader range of proteins. These developments enable comprehensive analysis of single-cell phenotypic characteristics and molecular responses, offering enhanced proteome coverage, measurement throughput, detection resolution, and quantitation accuracy through the use of integrated microfluidic chips. Here, we summarized the cutting-edge microfluidics-based methods for single-cell protein profiling, along with a detailed account of their technical metrics, including detection mode, multiplicity, throughput, and sensitivity. These specifications are conveniently summarized in Table 1. As illustrated in the table, a range of microfluidic single-cell protein analysis platforms have been developed and each method has its own unique advantages. At present, there is no gold standard method that significantly outperforms others across all aspects. Researchers must therefore consider factors such as the sample type, protein localization, sample throughput, and quantitative accuracy when selecting an appropriate single-cell protein analysis method for practical applications. Nonetheless, it is evident that the development trajectory of single-cell protein profiling using microfluidic technology is both clear and diverse: encompassing transitions from a few or dozens of cells to high-throughput single-cell analysis, from the characterization of one or a few target proteins to comprehensive proteomic analysis, from qualitative identification to quantitative analysis, and from single-omics to multi-omics integrated analysis.

With the emergence of single-cell protein profiling based on microfluidics, there remains a significant need for methodological improvements. The single-cell sample preparation is the first technical bottleneck for the current methodologies. Despite the long-standing development of single-cell analysis using microfluidics, achieving simultaneous high-throughput and high cell utilization remains a significant challenge for most platforms employing valve-, droplet-, well-, and field-based technologies. For example, DMF facilitates the preparation of single-cell protein samples with minimal cell loss, but this process is inherently constrained by its limited throughput. By contrast, droplet microfluidics breaks through the number of cells, while the proportion of available single-cell droplets is exceedingly low. Furthermore, the cellular proteome is variable and sensitive to sampling-related perturbations. These perturbations can alter the native cellular protein composition, potentially leading to inaccurate results in the subsequent analysis of the cellular state. In addition, protein loss during sample handling and transfer remains a serious challenge. Addressing these challenges requires the development of a highly integrated microfluidic chip featuring channels that enable contact-free, high-throughput single-cell processing and an interface that enables seamless integration with downstream analytical instrumentation. Such instrumentation must be capable of efficiently capturing, separating, labeling, and amplifying diverse proteins to enable high-quality single-cell protein profiling. Artificial intelligence-powered active matrix electrowetting-on-dielectric (AI-AM-EWOD) technology has emerged as a transformative platform for single-cell proteomic profiling.<sup>215,216</sup> This architecture

incorporates a high-density matrix of over 10 000 programmable electrodes, enabling precise droplet manipulation across thousands of individual cell analysis. The integration of AI-enhanced droplet control enables multiplexed, high-throughput operations with high-precision capabilities for single-cell proteomic profiling.

To enable a comprehensive analysis of cellular heterogeneity, single-cell protein profiling should not only be integrated with other omics approaches but also aligned with spatiotemporal information to precisely capture and resolve dynamic biological processes.

Incorporating spatiotemporal data within multicellular systems is crucial, offering unprecedented insights into dynamic gene regulation and cellular interaction networks at a resolution previously unattainable. For example, DBiT-seq<sup>217</sup> and its derivatives<sup>218–220</sup> developed by the Fan group introduced microfluidics into the spatial field, marking the advent of spatial multi-omics research. However, current spatial multi-omics technologies have not yet realized high-precision single-cell spatial sequencing at the single-cell level. Miniaturization, automation, and non-destructive integration of spatial-omics sample preparation *via* microfluidic platforms are considered highly promising approaches. Moreover, there are currently no reports on spatiotemporal multi-omics sequencing utilizing microfluidics. The integration of temporal labeling in tissues with spatial multi-omics could enable the construction of high-definition dynamic spatiotemporal landscape, offering an in-depth comprehension into the underlying mechanisms of biological processes on a time scale. Moreover, the integration of large, complex, and multimodal data of spatiotemporal multi-omics into specific biological models and mechanisms poses many challenges.

New streaming algorithms and high-performance software packages are necessary to advance methodologies to accommodate the growing volume of data produced by high-throughput and integrative analyses of single-cell multimodal data. Furthermore, these developed software tools have to possess the capability of integrating data across different modalities. Notwithstanding the technical complexities inherent to microfluidics-based single-cell protein profiling, it is poised to remain a pivotal driving force in the advancement of single-cell proteomics technology in the years to come. In the next decade, it is anticipated that a growing number of methodological innovations based on microfluidics in the field of single-cell protein profiling will emerge, thereby facilitating a more precise and thorough comprehension of the function and underlying mechanisms of the protein signalling network in biological processes.

## Author contributions

Conceptualization: Qingyu Ruan, Ruizhe Yang. Methodology: Qingyu Ruan, Ruizhe Yang, and Ye Tao. Visualization: Ruizhe Yang, Qingyu Ruan and Wenshang Guo. Writing – original draft: Ruizhe Yang, Qingyu Ruan, Wenshang Guo and Haicong Shen. Writing – review & editing: Ruizhe Yang,

Qingyu Ruan, Xiaoye Lin, Yingwen Chen, Chaoyong Yang, and Yukun Ren. Supervision: Yukun Ren, and Chaoyong Yang. Resources: Yukun Ren.

## Conflicts of interest

There are no conflicts to declare.

## Data availability

No primary research results, software or code have been included, and no new data were generated or analysed as part of this review.

## Acknowledgements

This work was financially supported by the National Natural Science Foundation of China (Grant No. 12072096), the Interdisciplinary Research Foundation of HIT (Grant No. IR2021229) and Excellent Youth Foundation of Heilongjiang Province of China (Grant No. YQ2024B006).

## References

- B. Huang, H. Wu, D. Bhaya, A. Grossman, S. Granier, B. K. Kobilka and R. N. Zare, *Science*, 2007, **315**, 81–84.
- P. Shahi, S. C. Kim, J. R. Haliburton, Z. J. Gartner and A. R. Abate, *Sci. Rep.*, 2017, **7**, 44447.
- S. T. Gebreyesus, A. A. Siyal, R. B. Kitata, E. S.-W. Chen, B. Enkhbayar, T. Angata, K.-I. Lin, Y.-J. Chen and H.-L. Tu, *Nat. Commun.*, 2022, **13**, 37.
- M. Wu, T. D. Perroud, N. Srivastava, C. S. Branda, K. L. Sale, B. D. Carson, K. D. Patel, S. S. Branda and A. K. Singh, *Lab Chip*, 2012, **12**, 2823–2831.
- X. Xu, M. Zhang, X. Zhang, Y. Liu, L. Cai, Q. Zhang, Q. Chen, L. Lin, S. Lin, Y. Song, Z. Zhu and C. Yang, *Anal. Chem.*, 2022, **94**, 8164–8173.
- H. H. Chang, M. Hemberg, M. Barahona, D. E. Ingber and S. Huang, *Nature*, 2008, **453**, 544–547.
- Y. Buganim, D. A. Faddah, A. W. Cheng, E. Itskovich, S. Markoulaki, K. Ganz, S. L. Klemm, A. van Oudenaarden and R. Jaenisch, *Cell*, 2012, **150**, 1209–1222.
- J. Cao, M. Spielmann, X. Qiu, X. Huang, D. M. Ibrahim, A. J. Hill, F. Zhang, S. Mundlos, L. Christiansen, F. J. Steemers, C. Trapnell and J. Shendure, *Nature*, 2019, **566**, 496–502.
- S. Valastyan and R. A. Weinberg, *Cell*, 2011, **147**, 275–292.
- M. Enge, H. E. Arda, M. Mignardi, J. Beausang, R. Bottino, S. K. Kim and S. R. Quake, *Cell*, 2017, **171**, 321–330.e314.
- L. Cai, L. Lin, S. Lin, X. Wang, Y. Chen, H. Zhu, Z. Zhu, L. Yang, X. Xu and C. Yang, *Small Methods*, 2024, **8**(12), e2400375.
- J. Wagner, M. A. Rapsomaniki, S. Chevrier, T. Anzeneder, C. Langwieder, A. Dykgers, M. Rees, A. Ramaswamy, S. Muenst, S. D. Soysal, A. Jacobs, J. Windhager, K. Silina, M. van den Broek, K. J. Dedes, M. Rodríguez Martínez, W. P. Weber and B. Bodenmiller, *Cell*, 2019, **177**, 1330–1345.e1318.
- A. A. Cohen, N. Geva-Zatorsky, E. Eden, M. Frenkel-Morgenstern, I. Issaeva, A. Sigal, R. Milo, C. Cohen-Saidon, Y. Liron, Z. Kam, L. Cohen, T. Danon, N. Perzov and U. Alon, *Science*, 2008, **322**, 1511.
- C. Kim, R. Gao, E. Sei, R. Brandt, J. Hartman, T. Hatschek, N. Crosetto, T. Foukakis and N. E. Navin, *Cell*, 2018, **173**, 879–893.e813.
- J. Cao, X. Chen, S. Huang, W. Shi, Q. Fan, Y. Gong, Y. Peng, L. Wu and C. Yang, *TrAC, Trends Anal. Chem.*, 2023, **158**, 116868.
- Z. Y. Li, M. Huang, X. K. Wang, Y. Zhu, J. S. Li, C. C. L. Wong and Q. Fang, *Anal. Chem.*, 2018, **90**, 5430–5438.
- L. Liu, H. Yang, D. Men, M. Wang, X. Gao, T. Zhang, D. Chen, C. Xue, Y. Wang, J. Wang and J. Chen, *Biosens. Bioelectron.*, 2020, **155**, 112097.
- J. George and J. Wang, *Anal. Chem.*, 2016, **88**, 10309–10315.
- Y. Zhu, G. Clair, W. B. Chrisler, Y. Shen, R. Zhao, A. K. Shukla, R. J. Moore, R. S. Misra, G. S. Pryhuber, R. D. Smith, C. Ansong and R. T. Kelly, *Angew. Chem., Int. Ed.*, 2018, **57**, 12370–12374.
- Y. Zhu, P. D. Piehowski, R. Zhao, J. Chen, Y. Shen, R. J. Moore, A. K. Shukla, V. A. Petyuk, M. Campbell-Thompson, C. E. Mathews, R. D. Smith, W. J. Qian and R. T. Kelly, *Nat. Commun.*, 2018, **9**, 882.
- C. Ma, R. Fan, H. Ahmad, Q. Shi, B. Comin-Anduix, T. Chodon, R. C. Koya, C. C. Liu, G. A. Kwong, C. G. Radu, A. Ribas and J. R. Heath, *Nat. Med.*, 2011, **17**, 738–743.
- F. Xu, H. Zhao, X. Feng, L. Chen, D. Chen, Y. Zhang, F. Nan, J. Liu and B.-F. Liu, *Angew. Chem., Int. Ed.*, 2014, **53**, 6730–6733.
- X. Yang, W. Liu, D. C.-H. Chan, S. U. Ahmed, H. Wang, Z. Wang, C. R. Nembr and S. O. Kelley, *J. Am. Chem. Soc.*, 2020, **142**, 14805–14809.
- N. Altemose, A. Maslan, C. Rios-Martinez, A. Lai, J. A. White and A. Streets, *Cell Syst.*, 2020, **11**, 354–366.e359.
- T. Khajvand, P. Huang, L. Li, M. Zhang, F. Zhu, X. Xu, M. Huang, C. Yang, Y. Lu and Z. Zhu, *Lab Chip*, 2021, **21**, 4823–4830.
- J. Lamanna, E. Y. Scott, H. S. Edwards, M. D. Chamberlain, M. D. M. Dryden, J. Peng, B. Mair, A. Lee, C. Chan, A. A. Sklavounos, A. Heffernan, F. Abbas, C. Lam, M. E. Olson, J. Moffat and A. R. Wheeler, *Nat. Commun.*, 2020, **11**, 5632.
- A. J. Hughes, D. P. Spelke, Z. Xu, C.-C. Kang, D. V. Schaffer and A. E. Herr, *Nat. Methods*, 2014, **11**, 749–755.
- T. Zhang, S. Li, A. R. Warden, B. Ghalandari, H. Li, X. Zhi, H. Xie and X. Ding, *Adv. Funct. Mater.*, 2020, **30**, 1910739.
- H. Xie, W. Guo, H. Jiang, T. Zhang, L. Zhao, J. Hu, S. Gao, S. Song, J. Xu, L. Xu, X. Sun, Y. Ding, L. Jiang and X. Ding, *Adv. Sci.*, 2024, 2308569.
- S. M. Prakadan, A. K. Shalek and D. A. Weitz, *Nat. Rev. Genet.*, 2017, **18**, 345–361.
- Y. Xu, K.-C. Wu, W. Jiang, Y. Hou, L. F. Cheow, V. H.-F. Lee and C.-H. Chen, *Anal. Chem.*, 2024, **96**, 49–58.
- M. N. Hsu, S.-C. Wei, S. Guo, D.-T. Phan, Y. Zhang and C.-H. Chen, *Small*, 2018, **14**, 1802918.
- C. Gawad, W. Koh and S. R. Quake, *Nat. Rev. Genet.*, 2016, **17**, 175–188.

- 34 A. A. Kolodziejczyk, J. K. Kim, V. Svensson, J. C. Marioni and S. A. Teichmann, *Mol. Cell*, 2015, **58**, 610–620.
- 35 Y. Bounab, K. Eyer, S. Dixneuf, M. Rybczynska, C. Chauvel, M. Mistretta, T. Tran, N. Aymerich, G. Chenon, J.-F. Llitjos, F. Venet, G. Monneret, I. A. Gillespie, P. Cortez, V. Moucadel, A. Pachot, A. Troesch, P. Leissner, J. Textoris, J. Bibette, C. Guyard, J. Baudry, A. D. Griffiths and C. Védrine, *Nat. Protoc.*, 2020, **15**, 2920–2955.
- 36 Y. Lu, Q. Xue, M. R. Eisele, E. S. Sulistijo, K. Brower, L. Han, A. D. Amirel, D. Pe'er, K. Miller-Jensen and R. Fan, *Proc. Natl. Acad. Sci. U. S. A.*, 2015, **112**, E607–E615.
- 37 H. Specht and N. Slavov, *J. Proteome Res.*, 2018, **17**, 2565–2571.
- 38 P. Zhao, S. Bhowmick, J. Yu and J. Wang, *Adv. Sci.*, 2018, **5**, 1800672.
- 39 R. Zenobi, *Science*, 2013, **342**, 1243259.
- 40 Y. Liu, X. Chen, Y. Zhang and J. Liu, *Analyst*, 2019, **144**, 846–858.
- 41 Y. Lu, L. Yang, W. Wei and Q. Shi, *Lab Chip*, 2017, **17**, 1250–1263.
- 42 J. Yu, J. Zhou, A. Sutherland, W. Wei, Y. S. Shin, M. Xue and J. R. Heath, *Annu. Rev. Anal. Chem.*, 2014, **7**, 275–295.
- 43 A. F. Altelaar, J. Munoz and A. J. Heck, *Nat. Rev. Genet.*, 2013, **14**, 35–48.
- 44 V. Espina, A. I. Mehta, M. E. Winters, V. Calvert, J. Wulfskuhle, E. F. Petricoin, 3rd and L. A. Liotta, *Proteomics*, 2003, **3**, 2091–2100.
- 45 S. Li, B. D. Plouffe, A. M. Belov, S. Ray, X. Wang, S. K. Murthy, B. L. Karger and A. R. Ivanov, *Mol. Cell. Proteomics*, 2015, **14**, 1672–1683.
- 46 Q. Chen, G. Yan, M. Gao and X. Zhang, *Anal. Chem.*, 2015, **87**, 6674–6680.
- 47 W. Chen, S. Wang, S. Adhikari, Z. Deng, L. Wang, L. Chen, M. Ke, P. Yang and R. Tian, *Anal. Chem.*, 2016, **88**, 4864–4871.
- 48 M. Wu and A. K. Singh, *Curr. Opin. Biotechnol.*, 2012, **23**, 83–88.
- 49 J. Guo, S. Wang, N. Dai, Y. N. Teo and E. T. Kool, *Proc. Natl. Acad. Sci. U. S. A.*, 2011, **108**, 3493–3498.
- 50 T. W. Murphy, Q. Zhang, L. B. Naler, S. Ma and C. Lu, *Analyst*, 2017, **143**, 60–80.
- 51 M. K. Steinbach, J. Leipert, T. Matzanke and A. Tholey, *Small Methods*, 2025, **9**, 2400495.
- 52 S. T. Gebreyesus, G. Muneer, C.-C. Huang, A. A. Siyal, M. Anand, Y.-J. Chen and H.-L. Tu, *Lab Chip*, 2023, **23**, 1726–1751.
- 53 V. N. Luk, L. K. Fiddes, V. M. Luk, E. Kumacheva and A. R. Wheeler, *Proteomics*, 2012, **12**, 1310–1318.
- 54 M. Khan, Y. Bi, G. Zhang, F. Yin, Y. Xie, L. Lin and Q. Hu, *TrAC, Trends Anal. Chem.*, 2023, **167**, 117257.
- 55 D. Anggraini, N. Ota, Y. Shen, T. Tang, Y. Tanaka, Y. Hosokawa, M. Li and Y. Yalikun, *Lab Chip*, 2022, **22**, 1438–1468.
- 56 Y. Chikaishi, K. Yoneda, T. Ohnaga and F. Tanaka, *Oncol. Rep.*, 2017, **37**, 77–82.
- 57 M. E. Warkiani, G. Guan, K. B. Luan, W. C. Lee, A. A. S. Bhagat, P. Kant Chaudhuri, D. S.-W. Tan, W. T. Lim, S. C. Lee, P. C. Y. Chen, C. T. Lim and J. Han, *Lab Chip*, 2014, **14**, 128–137.
- 58 E. Ozkumur, A. M. Shah, J. C. Ciciliano, B. L. Emmink, D. T. Miyamoto, E. Brachtel, M. Yu, P. I. Chen, B. Morgan, J. Trautwein, A. Kimura, S. Sengupta, S. L. Stott, N. M. Karabacak, T. A. Barber, J. R. Walsh, K. Smith, P. S. Spuhler, J. P. Sullivan, R. J. Lee, D. T. Ting, X. Luo, A. T. Shaw, A. Bardia, L. V. Sequist, D. N. Louis, S. Maheswaran, R. Kapur, D. A. Haber and M. Toner, *Sci. Transl. Med.*, 2013, **5**, 179ra147.
- 59 W.-P. Chou, H.-M. Wang, J.-H. Chang, T.-K. Chiu, C.-H. Hsieh, C.-J. Liao and M.-H. Wu, *Sens. Actuators, B*, 2017, **241**, 245–254.
- 60 J. Woo, S. M. Williams, L. M. Markillie, S. Feng, C.-F. Tsai, V. Aguilera-Vazquez, R. L. Sontag, R. J. Moore, D. Hu, H. S. Mehta, J. Cantlon-Bruce, T. Liu, J. N. Adkins, R. D. Smith, G. C. Clair, L. Pasa-Tolic and Y. Zhu, *Nat. Commun.*, 2021, **12**, 6246.
- 61 T. W. Murphy, Q. Zhang, L. B. Naler, S. Ma and C. Lu, *Analyst*, 2018, **143**, 60–80.
- 62 T. H. Nguyen, N. A. N. Thi, H. B. Thu, T. T. Bui, T. C. Duc and L. D. Quang, *Microfluid. Nanofluid.*, 2024, **28**, 35.
- 63 J. W. Hong and S. R. Quake, *Nat. Biotechnol.*, 2003, **21**, 1179–1183.
- 64 H. C. Fan, J. Wang, A. Potanina and S. R. Quake, *Nat. Biotechnol.*, 2011, **29**, 51–57.
- 65 A. S. Genshaft, S. Li, C. J. Gallant, S. Darmanis, S. M. Prakadan, C. G. K. Ziegler, M. Lundberg, S. Fredriksson, J. Hong, A. Regev, K. J. Livak, U. Landegren and A. K. Shalek, *Genome Biol.*, 2016, **17**, 188.
- 66 H. N. Joensson and H. A. Svahn, *Angew. Chem., Int. Ed.*, 2012, **51**, 12176–12192.
- 67 J. Lederberg, *J. Bacteriol.*, 1954, **68**, 258–259.
- 68 L. Huang, S. Bian, Y. Cheng, G. Shi, P. Liu, X. Ye and W. Wang, *Biomicrofluidics*, 2017, **11**(1), 011501.
- 69 Y. Zhou, Z. Yu, M. Wu, Y. Lan, C. Jia and J. Zhao, *Talanta*, 2023, **253**, 124044.
- 70 J. De Jonghe, T. S. Kaminski, D. B. Morse, M. Tabaka, A. L. Ellermann, T. N. Kohler, G. Amadei, C. E. Handford, G. M. Findlay, M. Zernicka-Goetz, S. A. Teichmann and F. Hollfelder, *Nat. Commun.*, 2023, **14**, 4788.
- 71 J. C. Love, J. L. Ronan, G. M. Grotenbreg, A. G. van der Veen and H. L. Ploegh, *Nat. Biotechnol.*, 2006, **24**, 703–707.
- 72 H. C. Fan, G. K. Fu and S. P. A. Fodor, *Science*, 2015, **347**(6222), 1258367.
- 73 Y. Lu, Q. Xue, M. R. Eisele, E. S. Sulistijo, K. Brower, L. Han, E.-a. D. Amir, D. Pe'er, K. Miller-Jensen and R. Fan, *Proc. Natl. Acad. Sci. U. S. A.*, 2015, **112**, E607–E615.
- 74 J. Gole, A. Gore, A. Richards, Y.-J. Chiu, H.-L. Fung, D. Bushman, H.-I. Chiang, J. Chun, Y.-H. Lo and K. Zhang, *Nat. Biotechnol.*, 2013, **31**(12), 1126–1132.
- 75 R. J. Jimenez-Valdes, R. Rodriguez-Moncayo, D. F. Cedillo-Alcantar and J. L. Garcia-Cordero, *Anal. Chem.*, 2017, **89**, 5210–5220.
- 76 L. Yang, Z. Wang, Y. Deng, Y. Li, W. Wei and Q. Shi, *Anal. Chem.*, 2016, **88**, 11077–11083.
- 77 S. H. Kim, T. Yamamoto, D. Fourmy and T. Fujii, *Small*, 2011, **7**, 3239–3247.

- 78 T. Luo, L. Fan, R. Zhu and D. Sun, *Micromachines*, 2019, **10**, 104.
- 79 N. N. Mohd Maidin, M. R. Buyong, R. A. Rahim and M. A. Mohamed, *Electrophoresis*, 2021, **42**, 2033–2059.
- 80 C. Wu, R. Chen, Y. Liu, Z. Yu, Y. Jiang and X. Cheng, *Lab Chip*, 2017, **17**, 4008–4014.
- 81 Y. L. Qin, L. Wu, T. Schneider, G. S. Yen, J. S. Wang, S. H. Xu, M. Li, A. L. Paguirigan, J. L. Smith, J. P. Radich, R. K. Anand and D. T. Chiu, *Angew. Chem., Int. Ed.*, 2018, **57**, 11378–11383.
- 82 M. Li and R. K. Anand, *J. Am. Chem. Soc.*, 2017, **139**, 8950–8959.
- 83 M. Li and R. K. Anand, *Chem. Sci.*, 2019, **10**, 1506–1513.
- 84 J.-L. He, A.-T. Chen, J.-H. Lee and S.-K. Fan, *Int. J. Mol. Sci.*, 2015, **16**, 22319–22332.
- 85 C. Yang, X. Gan, Y. Zeng, Z. Xu, L. Xu, C. Hu, H. Ma, B. Chai, S. Hu and Y. Chai, *Biosens. Bioelectron.*, 2023, **242**, 115723.
- 86 S. Hu, J. Ye, S. Shi, C. Yang, K. Jin, C. Hu, D. Wang and H. Ma, *Anal. Chem.*, 2023, **95**, 6905–6914.
- 87 Q. Ruan, W. Ruan, X. Lin, Y. Wang, F. Zou, L. Zhou, Z. Zhu and C. Yang, *Sci. Adv.*, 2020, **6**, eabd6454.
- 88 K. Samlali, F. Ahmadi, A. B. V. Quach, G. Soffer and S. C. C. Shih, *Small*, 2020, **16**, 2002400.
- 89 H. Wu, A. Wheeler and R. N. Zare, *Proc. Natl. Acad. Sci. U. S. A.*, 2004, **101**, 12809–12813.
- 90 Z. Zhang, X. Feng, F. Xu, X. Liu and B.-F. Liu, *Electrophoresis*, 2010, **31**, 3129–3136.
- 91 Z. Zhang, X. Feng, Q. Luo and B.-F. Liu, *Electrophoresis*, 2009, **30**, 3174–3180.
- 92 A. J. Dickinson, P. M. Armistead and N. L. Allbritton, *Anal. Chem.*, 2013, **85**, 4797–4804.
- 93 E. R. Mainz, Q. Wang, D. S. Lawrence and N. L. Allbritton, *Angew. Chem., Int. Ed.*, 2016, **55**, 13095–13098.
- 94 Q. Li, P. Chen, Y. Fan, X. Wang, K. Xu, L. Li and B. Tang, *Anal. Chem.*, 2016, **88**, 8610–8616.
- 95 D. Chen, F. Fan, X. Zhao, F. Xu, P. Chen, J. Wang, L. Ban, Z. Liu, X. Feng, Y. Zhang and B.-F. Liu, *Anal. Chem.*, 2016, **88**, 2466–2471.
- 96 M. Shi, X. Geng, C. Wang and Y. Guan, *Anal. Chem.*, 2019, **91**, 11493–11496.
- 97 H. Towbin, T. Staehelin and J. Gordon, *Proc. Natl. Acad. Sci. U. S. A.*, 1979, **76**, 4350–4354.
- 98 R. Ghosh, J. E. Gilda and A. V. Gomes, *Expert Rev. Proteomics*, 2014, **11**, 549–560.
- 99 C.-C. Kang, J.-M. G. Lin, Z. Xu, S. Kumar and A. E. Herr, *Anal. Chem.*, 2014, **86**, 10429–10436.
- 100 E. Rosàs-Canyelles, A. J. Modzelewski, A. Geldert, L. He and A. E. Herr, *Sci. Adv.*, 2020, **6**, eaay1751.
- 101 S. Li, Z. Wen, B. Ghalandari, T. Zhou, A. R. Warden, T. Zhang, P. Dai, Y. Yu, W. Guo, M. Liu, H. Xie and X. Ding, *Adv. Mater.*, 2021, **33**, 2101108.
- 102 S. M. Grist, A. P. Mourdoukoutas and A. E. Herr, *Nat. Commun.*, 2020, **11**, 6237.
- 103 T. A. Duncombe, C.-C. Kang, S. Maity, T. M. Ward, M. D. Pegram, N. Murthy and A. E. Herr, *Adv. Mater.*, 2016, **28**, 327–334.
- 104 G. Lomeli, M. Bosse, S. C. Bendall, M. Angelo and A. E. Herr, *Anal. Chem.*, 2021, **93**, 8517–8525.
- 105 J. Vlassakis and A. E. Herr, *Anal. Chem.*, 2015, **87**, 11030–11038.
- 106 B. Gumuscu and A. E. Herr, *Lab Chip*, 2020, **20**, 64–73.
- 107 E. Sinkala, E. Sollier-Christen, C. Renier, E. Rosàs-Canyelles, J. Che, K. Heirich, T. A. Duncombe, J. Vlassakis, K. A. Yamauchi, H. Huang, S. S. Jeffrey and A. E. Herr, *Nat. Commun.*, 2017, **8**, 14622.
- 108 A. Y. Fu, C. Spence, A. Scherer, F. H. Arnold and S. R. Quake, *Nat. Biotechnol.*, 1999, **17**, 1109–1111.
- 109 C. Buhlmann, T. Preckel, S. Chan, G. Luedke and M. Valer, *J. Biomol. Tech.*, 2003, **14**, 119–127.
- 110 D. Holmes and H. Morgan, *Anal. Chem.*, 2010, **82**, 1455–1461.
- 111 J. Wang, B. Fei, R. L. Geahlen and C. Lu, *Lab Chip*, 2010, **10**, 2673–2679.
- 112 T. Jing, Z. Lai, L. Wu, J. Han, C. T. Lim and C. H. Chen, *Anal. Chem.*, 2016, **88**, 11750–11757.
- 113 L. Liu, B. Fan, D. Wang, X. Li, Y. Song, T. Zhang, D. Chen, Y. Wang, J. Wang and J. Chen, *Micromachines*, 2018, **9**(11), 588.
- 114 X. Xuan, J. Zhu and C. Church, *Microfluid. Nanofluid.*, 2010, **9**, 1–16.
- 115 D. Spencer, G. Elliott and H. Morgan, *Lab Chip*, 2014, **14**, 3064–3073.
- 116 S. Etcheverry, A. Faridi, H. Ramachandraiah, T. Kumar, W. Margulis, F. Laurell and A. Russom, *Sci. Rep.*, 2017, **7**, 5628.
- 117 G. Holzner, B. Mateescu, D. van Leeuwen, G. Cereghetti, R. Dechant, S. Stavarakis and A. deMello, *Cell Rep.*, 2021, **34**(10), 108824.
- 118 E. Y. Basova and F. Foret, *Analyst*, 2015, **140**, 22–38.
- 119 D. J. Collins, A. Neild, A. deMello, A. Q. Liu and Y. Ai, *Lab Chip*, 2015, **15**, 3439–3459.
- 120 E. X. Ng, M. A. Miller, T. Jing and C. H. Chen, *Biosens. Bioelectron.*, 2016, **81**, 408–414.
- 121 H. Yang, Y. Wei, B. Fan, L. Liu, T. Zhang, D. Chen, J. Wang and J. Chen, *Microfluid. Nanofluid.*, 2021, **25**, 30.
- 122 H. Yang, G. Yang, T. Zhang, D. Chen, J. Wang and J. Chen, *J. Micromech. Microeng.*, 2022, **32**, 024002.
- 123 G. Yang, C. Gao, D. Chen, J. Wang, X. Huo and J. Chen, *Biomicrofluidics*, 2023, **17**, 064106.
- 124 J. U. Shim, L. F. Olguin, G. Whyte, D. Scott, A. Babbie, C. Abell, W. T. S. Huck and F. Hollfelder, *J. Am. Chem. Soc.*, 2009, **131**, 15251–15256.
- 125 E. Brouzes, M. Medkova, N. Savenelli, D. Marran, M. Twardowski, J. B. Hutchison, J. M. Rothberg, D. R. Link, N. Perrimon and M. L. Samuels, *Proc. Natl. Acad. Sci. U. S. A.*, 2009, **106**, 14195–14200.
- 126 L. Mazutis, J. Gilbert, W. L. Ung, D. A. Weitz, A. D. Griffiths and J. A. Heyman, *Nat. Protoc.*, 2013, **8**, 870–891.
- 127 B. L. Wang, A. Ghaderi, H. Zhou, J. Agresti, D. A. Weitz, G. R. Fink and G. Stephanopoulos, *Nat. Biotechnol.*, 2014, **32**, 473–478.
- 128 E. X. Ng, M. A. Miller, T. Jing and C.-H. Chen, *Biosens. Bioelectron.*, 2016, **81**, 408–414.
- 129 N. Shembekar, H. Hu, D. Eustace and C. A. Merten, *Cell Rep.*, 2018, **22**, 2206–2215.

- 130 V. Chokkalingam, J. Tel, F. Wimmers, X. Liu, S. Semenov, J. Thiele, C. G. Figdor and W. T. Huck, *Lab Chip*, 2013, **13**, 4740–4744.
- 131 L. Cong, J. Wang, X. Li, Y. Tian, S. Xu, C. Liang, W. Xu, W. Wang and S. Xu, *Anal. Chem.*, 2022, **94**, 10375–10383.
- 132 Y. S. Shin, H. Ahmad, Q. Shi, H. Kim, T. A. Pascal, R. Fan, W. A. Goddard, 3rd and J. R. Heath, *ChemPhysChem*, 2010, **11**, 3063–3069.
- 133 Y. Lu, J. J. Chen, L. Mu, Q. Xue, Y. Wu, P. H. Wu, J. Li, A. O. Vortmeyer, K. Miller-Jensen, D. Wirtz and R. Fan, *Anal. Chem.*, 2013, **85**, 2548–2556.
- 134 S. M. Schubert, S. R. Walter, M. Manesse and D. R. Walt, *Anal. Chem.*, 2016, **88**, 2952–2957.
- 135 Q. Li, S. A. Bencherif and M. Su, *Anal. Chem.*, 2021, **93**, 10292–10300.
- 136 V. Herrera, S.-C. J. Hsu, M. K. Rahim, C. Chen, L. Nguyen, W. F. Liu and J. B. Haun, *Analyst*, 2019, **144**, 980–989.
- 137 V. Herrera, S.-C. J. Hsu, V. Y. Naveen, W. F. Liu and J. B. Haun, *Anal. Chem.*, 2022, **94**, 658–668.
- 138 S. Ansaryan, Y.-C. Liu, X. Li, A. M. Economou, C. S. Eberhardt, C. Jandus and H. Altug, *Nat. Biomed. Eng.*, 2023, **7**, 943–958.
- 139 C. Wang, C. Wang, Y. Wu, J. Gao, Y. Han, Y. Chu, L. Qiang, J. Qiu, Y. Gao, Y. Wang, F. Song, Y. Wang, X. Shao, Y. Zhang and L. Han, *Adv. Healthcare Mater.*, 2022, **11**, 2102800.
- 140 F. Song, C. Wang, C. Wang, J. Wang, Y. Wu, Y. Wang, H. Liu, Y. Zhang and L. Han, *Small Methods*, 2022, **6**, 2200717.
- 141 L. Yang, Z. Wang, Y. Deng, Y. Li, W. Wei and Q. Shi, *Anal. Chem.*, 2016, **88**, 11077–11083.
- 142 L. Yang, A. Ball, J. Liu, T. Jain, Y.-M. Li, F. Akhter, D. Zhu and J. Wang, *Nat. Commun.*, 2022, **13**, 3548.
- 143 L. Xu, H. Xie, B. Wang, Z. Zhu, H. Jiang, X. Duan, S. Deng, J. Xu, L. Jiang and X. Ding, *Anal. Chem.*, 2023, **95**, 11399–11409.
- 144 X. Wu, X. Lin, X. Ma, H. Huang, D. Zhang, Y. Liu, R. Cheng, J. Song, L. Zhang, Y. Tan, R. Peng, T. Bing, Q. Wu and W. Tan, *J. Am. Chem. Soc.*, 2025, **147**, 20394–20405.
- 145 P. Maschmeyer and S. Haas, *Mol. Cell*, 2022, **82**, 234–236.
- 146 Y. Ma, K. Chen, F. Xia, R. Atwal, H. Wang, S. U. Ahmed, L. Cardarelli, I. Lui, B. Duong, Z. Wang, J. A. Wells, S. S. Sidhu and S. O. Kelley, *ACS Nano*, 2021, **15**, 19202–19210.
- 147 X. Zhang, X. Wei, C.-X. Wu, X. Men, J. Wang, J.-J. Bai, X.-Y. Sun, Y. Wang, T. Yang, C. T. Lim, M.-L. Chen and J.-H. Wang, *ACS Nano*, 2024, **18**, 6612–6622.
- 148 T. E. Angel, U. K. Aryal, S. M. Hengel, E. S. Baker, R. T. Kelly, E. W. Robinson and R. D. Smith, *Chem. Soc. Rev.*, 2012, **41**, 3912–3928.
- 149 P. Feist and A. B. Hummon, *Int. J. Mol. Sci.*, 2015, **16**, 3537–3563.
- 150 H. B. Gutstein, J. S. Morris, S. P. Annangudi and J. V. Sweedler, *Mass Spectrom. Rev.*, 2008, **27**, 316–330.
- 151 Y. Zhu, P. D. Piehowski, R. Zhao, J. Chen, Y. Shen, R. J. Moore, A. K. Shukla, V. A. Petyuk, M. Campbell-Thompson, C. E. Mathews, R. D. Smith, W.-J. Qian and R. T. Kelly, *Nat. Commun.*, 2018, **9**, 882.
- 152 E. M. Schoof, B. Furtwängler, N. Üresin, N. Rapin, S. Savickas, C. Gentil, E. Lechman, U. a. d. Keller, J. E. Dick and B. T. Porse, *Nat. Commun.*, 2021, **12**, 3341.
- 153 Y. Cong, K. Motamedchaboki, S. A. Misal, Y. Liang, A. J. Guise, T. Truong, R. Huguet, E. D. Plowey, Y. Zhu, D. Lopez-Ferrer and R. T. Kelly, *Chem. Sci.*, 2021, **12**, 1001–1006.
- 154 N. Slavov, *Curr. Opin. Chem. Biol.*, 2021, **60**, 1–9.
- 155 P. Zhao, Y. Feng, J. Wu, J. Zhu, J. Yang, X. Ma, Z. Ouyang, X. Zhang, W. Zhang and W. Wang, *Anal. Chem.*, 2023, **95**, 7212–7219.
- 156 Z. Ye, P. Sabatier, L. van der Hoeven, M. Y. Lechner, T. Phlairaarn, U. H. Guzman, Z. Liu, H. Huang, M. Huang, X. Li, D. Hartlmayr, F. Izaguirre, A. Seth, H. J. Joshi, S. Rodin, K.-H. Grinnemo, O. B. Hørning, D. B. Bekker-Jensen, N. Bache and J. V. Olsen, *Nat. Methods*, 2025, **22**, 499–509.
- 157 V. Petrosius, P. Aragon-Fernandez, T. N. Arrey, J. Woessmann, N. Üresin, B. de Boer, J. Su, B. Furtwängler, H. Stewart, E. Denisov, J. Petzoldt, A. C. Peterson, C. Hock, E. Damoc, A. Makarov, V. Zabrouskov, B. T. Porse and E. M. Schoof, *Mol. Cell. Proteomics*, 2025, **24**, 100982.
- 158 M. Yang, R. Nelson and A. Ros, *Anal. Chem.*, 2016, **88**, 6672–6679.
- 159 M. Yang, J. Cruz Villarreal, N. Ariyasinghe, R. Kruithoff, R. Ros and A. Ros, *Anal. Chem.*, 2021, **93**, 6053–6061.
- 160 J. Cruz Villarreal, R. Kruithoff, A. Egatz-Gomez, P. D. Coleman, R. Ros, T. R. Sandrin and A. Ros, *Anal. Bioanal. Chem.*, 2022, **414**, 3945–3958.
- 161 C. Ctorteccka, N. M. Clark, B. W. Boyle, A. Seth, D. R. Mani, N. D. Udeshi and S. A. Carr, *Nat. Commun.*, 2024, **15**, 5707.
- 162 R. Ishibashi, K. Mawatari and T. Kitamori, *J. Chromatogr. A*, 2012, **1238**, 152–155.
- 163 J. Wang, B. Xue, O. Awoyemi, H. Yuliantoro, L. T. Mendis, A. DeVor, S. J. Valentine and P. Li, *Anal. Chim. Acta*, 2024, **1329**, 343241.
- 164 J. Woo, S. M. Williams, L. M. Markillie, S. Feng, C.-F. Tsai, V. Aguilera-Vazquez, R. L. Sontag, R. J. Moore, D. Hu, H. S. Mehta, J. Cantlon-Bruce, T. Liu, J. N. Adkins, R. D. Smith, G. C. Clair, L. Pasa-Tolic and Y. Zhu, *Nat. Commun.*, 2021, **12**, 6246.
- 165 A. Leduc, L. Khoury, J. Cantlon, S. Khan and N. Slavov, *Nat. Protoc.*, 2024, **19**, 3750–3776.
- 166 I. Barbulovic-Nad, H. Yang, P. S. Park and A. R. Wheeler, *Lab Chip*, 2008, **8**, 519–526.
- 167 A. R. Wheeler, H. Moon, C.-J. C. Kim, J. A. Loo and R. L. Garrell, *Anal. Chem.*, 2004, **76**, 4833–4838.
- 168 A. R. Wheeler, H. Moon, C. A. Bird, R. R. Ogorzalek Loo, C.-J. C. J. Kim, J. A. Loo and R. L. Garrell, *Anal. Chem.*, 2005, **77**, 534–540.
- 169 H. Moon, A. R. Wheeler, R. L. Garrell, J. A. Loo and C.-J. C. Kim, *Lab Chip*, 2006, **6**, 1213–1219.
- 170 V. N. Luk and A. R. Wheeler, *Anal. Chem.*, 2009, **81**, 4524–4530.
- 171 J. Leipert and A. Tholey, *Lab Chip*, 2019, **19**, 3490–3498.
- 172 M. K. Steinbach, J. Leipert, C. Blurton, M. Leippe and A. Tholey, *J. Proteome Res.*, 2022, **21**, 1986–1996.

- 173 J. Leipert, M. K. Steinbach and A. Tholey, *Anal. Chem.*, 2021, **93**, 6278–6286.
- 174 J. Peng, C. Chan, S. Zhang, A. A. Sklavounos, M. E. Olson, E. Y. Scott, Y. Hu, V. Rajesh, B. B. Li, M. D. Chamberlain, S. Zhang, H. Peng and A. R. Wheeler, *Chem. Sci.*, 2023, **14**, 2887–2900.
- 175 Z. Yang, K. Jin, Y. Chen, Q. Liu, H. Chen, S. Hu, Y. Wang, Z. Pan, F. Feng, M. Shi, H. Xie, H. Ma and H. Zhou, *JACS Au*, 2024, **4**, 1811–1823.
- 176 A. Thompson, J. Schäfer, K. Kuhn, S. Kienle, J. Schwarz, G. Schmidt, T. Neumann and C. Hamon, *Anal. Chem.*, 2003, **75**, 1895–1904.
- 177 W. Zhang, J. Zhang, C. Xu, N. Li, H. Liu, J. Ma, Y. Zhu and H. Xie, *Proteomics*, 2012, **12**, 3475–3484.
- 178 B. C. Searle, K. E. Swearingen, C. A. Barnes, T. Schmidt, S. Gessulat, B. Küster and M. Wilhelm, *Nat. Commun.*, 2020, **11**, 1548.
- 179 B. Y. Fan, J. B. Wang, Y. Xu and J. Chen, in *Computational Systems Biology: Methods And Protocols*, ed. T. Huang, 2018, vol. 1754, pp. 293–309.
- 180 T. J. Comi, T. D. Do, S. S. Rubakhin and J. V. Sweedler, *J. Am. Chem. Soc.*, 2017, **139**, 3920–3929.
- 181 E. Landhuis, *Nature*, 2018, **557**, 595–597.
- 182 L. Gu, C. Li, J. Aach, D. E. Hill, M. Vidal and G. M. Church, *Nature*, 2014, **515**, 554–557.
- 183 Y. Song, X. Xu, W. Wang, T. Tian, Z. Zhu and C. Yang, *Analyst*, 2019, **144**, 3172–3189.
- 184 Z. Li, H. Cheng, S. Shao, X. Lu, L. Mo, J. Tsang, P. Zeng, Z. Guo, S. Wang, D. A. Nathanson, J. R. Heath, W. Wei and M. Xue, *Angew. Chem., Int. Ed.*, 2018, **57**, 11554–11558.
- 185 M. Xue, W. Wei, Y. Su, J. Kim, Y. S. Shin, W. X. Mai, D. A. Nathanson and J. R. Heath, *J. Am. Chem. Soc.*, 2015, **137**, 4066–4069.
- 186 A. M. Xu, Q. Liu, K. L. Takata, S. Jeoung, Y. Su, I. Antoshechkin, S. Chen, M. Thomson and J. R. Heath, *Lab Chip*, 2018, **18**, 3251–3262.
- 187 E. Z. Macosko, A. Basu, R. Satija, J. Nemes, K. Shekhar, M. Goldman, I. Tirosh, A. R. Bialas, N. Kamitaki, E. M. Martersteck, J. J. Trombetta, D. A. Weitz, J. R. Sanes, A. K. Shalek, A. Regev and S. A. McCarroll, *Cell*, 2015, **161**, 1202–1214.
- 188 V. M. Peterson, K. X. Zhang, N. Kumar, J. Wong, L. Li, D. C. Wilson, R. Moore, T. K. McClanahan, S. Sadekova and J. A. Klappenbach, *Nat. Biotechnol.*, 2017, **35**, 936–939.
- 189 M. Stoeckius, C. Hafemeister, W. Stephenson, B. Houck-Loomis, P. K. Chattopadhyay, H. Swerdlow, R. Satija and P. Smibert, *Nat. Methods*, 2017, **14**, 865–868.
- 190 E. P. Mimitou, A. Cheng, A. Montalbano, S. Hao, M. Stoeckius, M. Legut, T. Roush, A. Herrera, E. Papalex, Z. Ouyang, R. Satija, N. E. Sanjana, S. B. Koralov and P. Smibert, *Nat. Methods*, 2019, **16**, 409–412.
- 191 E. P. Mimitou, C. A. Lareau, K. Y. Chen, A. L. Zorzetto-Fernandes, Y. Hao, Y. Takeshima, W. Luo, T.-S. Huang, B. Z. Yeung, E. Papalex, P. I. Thakore, T. Kibayashi, J. B. Wing, M. Hata, R. Satija, K. L. Nazer, S. Sakaguchi, L. S. Ludwig, V. G. Sankaran, A. Regev and P. Smibert, *Nat. Biotechnol.*, 2021, **39**, 1246–1258.
- 192 E. Swanson, C. Lord, J. Reading, A. T. Heubeck, P. C. Genge, Z. Thomson, M. D. A. Weiss, X.-j. Li, A. K. Savage, R. R. Green, T. R. Torgerson, T. F. Bumol, L. T. Graybuck and P. J. Skene, *eLife*, 2021, **10**, e63632.
- 193 M. Junkin, Alicia J. Kaestli, Z. Cheng, C. Jordi, C. Albayrak, A. Hoffmann and S. Tay, *Cell Rep.*, 2016, **15**, 411–422.
- 194 K. Rooijers, C. M. Markodimitraki, F. J. Rang, S. S. de Vries, A. Chialastri, K. L. de Luca, D. Mooijman, S. S. Dey and J. Kind, *Nat. Biotechnol.*, 2019, **37**, 766–772.
- 195 S.-Q. Zhang, K.-Y. Ma, A. A. Schonnesen, M. Zhang, C. He, E. Sun, C. M. Williams, W. Jia and N. Jiang, *Nat. Biotechnol.*, 2018, **36**, 1156–1159.
- 196 G. X. Y. Zheng, J. M. Terry, P. Belgrader, P. Ryvkin, Z. W. Bent, R. Wilson, S. B. Ziraldo, T. D. Wheeler, G. P. McDermott, J. Zhu, M. T. Gregory, J. Shuga, L. Montesclaros, J. G. Underwood, D. A. Masquelier, S. Y. Nishimura, M. Schnall-Levin, P. W. Wyatt, C. M. Hindson, R. Bharadwaj, A. Wong, K. D. Ness, L. W. Beppu, H. J. Deeg, C. McFarland, K. R. Loeb, W. J. Valente, N. G. Ericson, E. A. Stevens, J. P. Radich, T. S. Mikkelsen, B. J. Hindson and J. H. Bieleas, *Nat. Commun.*, 2017, **8**, 14049.
- 197 M. Xue, W. Wei, Y. Su, J. Kim, Y. S. Shin, W. X. Mai, D. A. Nathanson and J. R. Heath, *J. Am. Chem. Soc.*, 2015, **137**, 4066–4069.
- 198 M. Xue, W. Wei, Y. Su, D. Johnson and J. R. Heath, *J. Am. Chem. Soc.*, 2016, **138**, 3085–3093.
- 199 N. Slavov, *Development*, 2023, **150**, dev201492.
- 200 Y. Liu, A. Beyer and R. Aebersold, *Cell*, 2016, **165**, 535–550.
- 201 A. Momenzadeh and J. G. Meyer, *Cell Genomics*, 2025, **5**, 100973.
- 202 V. M. Peterson, K. X. Zhang, N. Kumar, J. Wong, L. Li, D. C. Wilson, R. Moore, T. K. McClanahan, S. Sadekova and J. A. Klappenbach, *Nat. Biotechnol.*, 2017, **35**, 936–939.
- 203 M. Stoeckius, C. Hafemeister, W. Stephenson, B. Houck-Loomis, P. K. Chattopadhyay, H. Swerdlow, R. Satija and P. Smibert, *Nat. Methods*, 2017, **14**, 865–868.
- 204 S. C. Bendall, E. F. Simonds, P. Qiu, E.-a. D. Amir, P. O. Krutzik, R. Finck, R. V. Bruggner, R. Melamed, A. Trejo, O. I. Ornatsky, R. S. Balderas, S. K. Plevritis, K. Sachs, D. Pe'er, S. D. Tanner and G. P. Nolan, *Science*, 2011, **332**, 687–696.
- 205 V. Knight, *J. Immunol. Methods*, 2025, **537**, 113818.
- 206 J. C. Love, J. L. Ronan, G. M. Grotenbreg, A. G. van der Veen and H. L. Ploegh, *Nat. Biotechnol.*, 2006, **24**, 703–707.
- 207 Q. Han, E. M. Bradshaw, B. Nilsson, D. A. Hafner and J. C. Love, *Lab Chip*, 2010, **10**, 1391–1400.
- 208 Y. Luo and H. Liang, *Trends Genet.*, 2023, **39**, 758–772.
- 209 L. Kuett, R. Catena, A. Özcan, A. Plüss, H. R. Ali, M. A. Sa'd, S. Alon, S. Aparicio, G. Battistoni, S. Balasubramanian, R. Becker, B. Bodenmiller, E. S. Boyden, D. Bressan, A. Bruna, M. Burger, C. Caldas, M. Callari, I. G. Cannell, H. Casbolt, N. Chornay, Y. Cui, A. Dariush, K. Dinh, A. Emenari, Y. Eyal-Lubling, J. Fan, A. Fatemi, E. Fisher, E. A. González-Solares, C. González-Fernández, D. Goodwin, W. Greenwood, F. Grimaldi, G. J. Hannon, S. Harris, C. Jauset, J. A. Joyce, E. D. Karagiannis, T. Kovačević, L. Kuett, R. Kunes, A. K. Yoldaş, D. Lai, E. Laks, H. Lee, M. Lee, G. Lerda, Y. Li, A. McPherson, N. Millar, C. M. Mulvey, I.

- Nugent, C. H. O'Flanagan, M. Paez-Ribes, I. Pearsall, F. Qosaj, A. J. Roth, O. M. Rueda, T. Ruiz, K. Sawicka, L. A. Sepúlveda, S. P. Shah, A. Shea, A. Sinha, A. Smith, S. Tavaré, S. Tietscher, I. Vázquez-García, S. L. Vogl, N. A. Walton, A. T. Wassie, S. S. Watson, J. Weselak, S. A. Wild, E. Williams, J. Windhager, C. Xia, P. Zheng, X. Zhuang, P. Schraml, H. Moch, N. de Souza, B. Bodenmiller and I. C. Cancer Grand Challenges, *Nat. Cancer*, 2022, **3**, 122–133.
- 210 T. Guo, J. A. Steen and M. Mann, *Nature*, 2025, **638**, 901–911.
- 211 J. A. Lee, J. Spidlen, K. Boyce, J. Cai, N. Crosbie, M. Dalphin, J. Furlong, M. Gasparetto, M. Goldberg, E. M. Goralczyk, B. Hyun, K. Jansen, T. Kollmann, M. Kong, R. Leif, S. McWeeney, T. D. Moloshok, W. Moore, G. Nolan, J. Nolan, J. Nikolich-Zugich, D. Parrish, B. Purcell, Y. Qian, B. Selvaraj, C. Smith, O. Tchuvatkina, A. Wertheimer, P. Wilkinson, C. Wilson, J. Wood, R. Zigon, R. H. Scheuermann and R. R. Brinkman, *Cytometry, Part A*, 2008, **73A**, 926–930.
- 212 T. Kalina, J. Flores-Montero, V. H. J. van der Velden, M. Martin-Ayuso, S. Böttcher, M. Ritgen, J. Almeida, L. Lhermitte, V. Asnafi, A. Mendonça, R. de Tute, M. Cullen, L. Sedek, M. B. Vidriales, J. J. Pérez, J. G. te Marvelde, E. Mejstrikova, O. Hrusak, T. Szczepański, J. J. M. van Dongen, A. Orfao and C. on behalf of the EuroFlow, *Leukemia*, 2012, **26**, 1986–2010.
- 213 V. Iyer, Z. Yang, J. Ko, R. Weissleder and D. Issadore, *Lab Chip*, 2022, **22**, 3110–3121.
- 214 M. Chauhan, S. Kumar, A. Biswas, M. Kumar, S. K. Verma, A. Mishra, V. Singh, A. C. Bisen, S. Agrawal, A. D. Choudhury, R. Rayiti and R. S. Bhatta, *Lett. Drug Des. Discovery*, 2024, **21**, 3319–3331.
- 215 D. Wang, K. Jin, J. Ji, C. Hu, M. Du, Y. Belgaid, S. Shi, J. Li, S. Hu, A. Nathan, J. Yu and H. Ma, *iScience*, 2024, **27**(5), 109324.
- 216 Z. Jia, C. Chang, S. Hu, J. Li, M. Ge, W. Dong and H. Ma, *Microsyst. Nanoeng.*, 2024, **10**, 139.
- 217 Y. Liu, M. Yang, Y. Deng, G. Su, A. Enniful, C. C. Guo, T. Tebaldi, D. Zhang, D. Kim, Z. Bai, E. Norris, A. Pan, J. Li, Y. Xiao, S. Halene and R. Fan, *Cell*, 2020, **183**, 1665–1681. e1618.
- 218 Y. Deng, M. Bartosovic, P. Kukanja, D. Zhang, Y. Liu, G. Su, A. Enniful, Z. Bai, G. Castelo-Branco and R. Fan, *Science*, 2022, **375**, 681–686.
- 219 Y. Liu, M. DiStasio, G. Su, H. Asashima, A. Enniful, X. Qin, Y. Deng, J. Nam, F. Gao, P. Bordignon, M. Cassano, M. Tomayko, M. Xu, S. Halene, J. E. Craft, D. Hafler and R. Fan, *Nat. Biotechnol.*, 2023, **41**, 1405–1409.
- 220 D. Zhang, Y. Deng, P. Kukanja, E. Agirre, M. Bartosovic, M. Dong, C. Ma, S. Ma, G. Su, S. Bao, Y. Liu, Y. Xiao, G. B. Rosoklija, A. J. Dwork, J. J. Mann, K. W. Leong, M. Boldrini, L. Wang, M. Haeussler, B. J. Raphael, Y. Kluger, G. Castelo-Branco and R. Fan, *Nature*, 2023, **616**, 113–122.